TABLE OF CONTENTS

LIST OF FIGURES....2
LIST OF ABBREVIATIONS, ACRONYMS AND DEFINITION OF TERMS....3
1 INTRODUCTION....4
2 LIST OF REFERENCES....5

[redacted]

Confidential

LIST OF FIGURES

Figure 2.6.1: 1 Chemical Structure of MOV 4

LIST OF ABBREVIATIONS, ACRONYMS AND DEFINITION OF TERMS

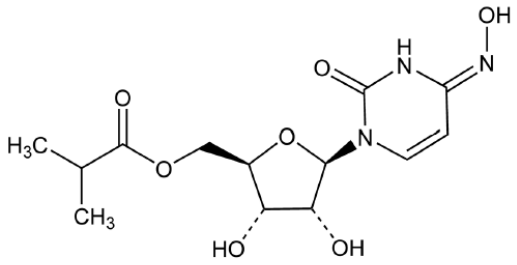
Abbreviation/Acronym	Definition
COVID-19	Coronavirus disease 2019
EIDD	Emory Institute for Drug Development
IUPAC	International Union of Pure and Applied Chemistry
MERS	Middle east respiratory syndrome
MERS-CoV	MERS coronavirus
MHV	Mouse hepatitis virus
MOV	Molnupiravir (MK-4482, EIDD-2801)
NHC	N-hydroxycytidine (EIDD-1931)
NHC-TP	N-hydroxycytidine-5′-triphosphate (EIDD-2061)
Q12H	Every 12 hours
RdRp	RNA-dependent RNA polymerase
RNA	Ribonucleic acid
SARS	Severe acute respiratory syndrome
SARS-CoV-2	SARS-associated coronavirus-2
WA1	SARS-CoV-2, Isolate USA-WA1/2020

1 INTRODUCTION

Molnupiravir (MOV; MK-4482) is the 5′-isobutyrate prodrug of the broadly active, antiviral ribonucleoside analog N-hydroxycytidine (NHC) developed for the oral treatment of adult patients with COVID-19. MOV is hydrolyzed by esterases either during or after absorption to deliver NHC into systemic circulation. Once distributed inside cells, NHC is phosphorylated to its corresponding triphosphate anabolite (NHC-TP) and acts as a competitive alternative substrate for virally encoded RdRp. MOV and NHC inhibit replication of viral pathogens from multiple RNA virus families, including pathogenic coronaviruses such as SARS-CoV-2. Antiviral activity has been verified in animal models of coronavirus virus infection.

The chemical structure of MOV is presented in [Figure 2.6.1: 1].

Figure 2.6.1: 1 Chemical Structure of MOV



Chemical Name (IUPAC): {(2*R*,3*S*,4*R*,5*R*)-3,4-Dihydroxy-5-[(4*Z*)-4-(hydroxyimino)-2-oxo-3,4-dihydropyrimidin-1(2*H*)-yl]oxolan-2-yl}methyl 2-methylpropanoate

Molecular Formula: $C_{13}H_{19}N_3O_7$

Molecular Weight: 329.31 g/mol

Coronaviruses are a family of enveloped positive-strand RNA viruses, which include SARS-CoV and MERS-CoV, that primarily target the respiratory system in humans and animals [Ref. 4.3: 05JRQN]. COVID-19 disease, caused by the novel SARS-CoV-2 virus, was first reported in December 2019. Patients presented with severe acute pneumonia of unknown microbial etiology, which was later isolated and identified as a new coronavirus designated SARS-CoV-2. COVID-19 is a potentially fatal disease that is of great global public health concern [Ref. 4.3: 05JRQN]. SARS-CoV-2 spread rapidly to more than 200 countries and territories worldwide [Ref. 4.3: 05JSVX]. COVID-19 was declared a global pandemic by the World Health Organization on 11-MAR-2020. The situation has continued to evolve rapidly, with new epidemiologic and clinical data available daily.

MOV, an oral direct-acting antiviral agent, will address the critical need for different therapeutic agents to treat COVID-19. MOV is administered orally enabling patients to initiate therapy in an outpatient setting. This flexibility in outpatient management would help to limit direct patient interactions with health care staff and decrease transmission risk, which

C Confidential

is significant due to the highly contagious nature of SARS-CoV-2. In vitro, NHC has a high genetic barrier to the development of resistance in nonclinical models and retains activity against SARS-CoV-2 and MHV (a related coronavirus) harbouring remdesivir resistance-associated mutations in the viral polymerase. In vitro, MOV shows broad-spectrum activity against multiple viruses including coronaviruses SARS-CoV-2, SARS-CoV, and MERS-CoV. NHC is also active against the original SARS-CoV-2 WA1 isolate as well as the emergent SARS-CoV-2 variants of concern B.1.1.7 (Alpha), B.1.351 (Beta), P.1 (Gamma), B.1.617.2 (Delta), B.1.1.529 (Omicron), and BA.1.1 (Omicron), variant of interest C.37 (Lambda), and variant being monitored B.1.621 (Mu).The recommended dose of MOV in adult patients is 800 mg Q12H for 5 days.

Nonclinical pharmacology, pharmacokinetic, and toxicology studies are summarized in the respective 2.6 modules. The results from this comprehensive nonclinical evaluation, as well as the results of the clinical assessment indicate that MOV has the efficacy and safety profile to fulfill this significant and urgent medical need for the treatment of COVID-19.

2 LIST OF REFERENCES

[Ref. 4.3: 05JRQN] Gorbalenya AE, Baker SC, Baric RS, de Groot RJ, Drosten C, Gulyaeva AA, et al. The species Severe acute respiratory syndrome-related coronavirus: classifying 2019-nCoV and naming it SARS-CoV-2. Nat Microbiol. 2020 Mar;5:536-44.

[Ref. 4.3: 05JSVX] World health Organization. Coronavirus disease (COVID-19): situation report - 171. Geneva (Switzerland): World Health Organization (WHO); 2020. 18 p.

[redacted]

C Confidential

TABLE OF CONTENTS

TABLE OF CONTENTS 1
LIST OF TABLES 3
LIST OF FIGURES 4
LIST OF ABBREVIATIONS, ACRONYMS AND DEFINITION OF TERMS 5
1 BRIEF SUMMARY 9
2 PRIMARY PHARMACODYNAMICS 15
2.1 In Vitro Pharmacology 15
2.1.1 Mechanism of Action 15
2.1.2 Antiviral Activity of NHC In Vitro 16
2.1.3 In Vitro Antiviral Activity of NHC Against SARS-CoV-2 Variants of Concern and Variants of Interest 22
2.1.4 In Vitro Activity of NHC Against SARS-CoV-2 With Remdesivir Resistance-associated and MOV Treatment-emergent Amino Acid Substitutions in NSP12 (Polymerase) and NSP14 (Exonuclease) 26
2.1.5 NHC Resistance Selection Studies and Antiviral Activity Against Remdesivir-resistant Mouse Hepatitis Virus Model Coronavirus and SARS-CoV 29
2.1.5.1 NHC Resistance Selection Against MHV and MERS-CoV 29
2.1.5.2 NHC Activity Against Remdesivir-resistant Viruses 29
2.1.6 In Vitro Evaluation of NHC Uptake by Cell Lines, by Human, Dog, and Rat PBMCs and in HBEC Air-liquid Interface Cultures 31
2.1.7 Cytotoxicity of NHC in Tissue Culture Utilizing Cells From Different Organs and Species 32
2.1.8 Assessment of Mitochondrial Toxicity 33
2.1.9 In Vitro Evaluation of MOV on Human Myeloid and Erythroid Colony Forming Cell Assays (PD006) 33
2.2 In Vivo Pharmacology 34
2.2.1 MOV Activity Against SARS-CoV-2 in a Pre-exposure Prophylaxis and Post-exposure Therapeutics Lung Only Mouse Model 34
2.2.2 Activity Against SARS-CoV-2 in a Ferret Model of Coronavirus Infection 35
2.2.3 MOV Reduces SARS-CoV-2 Viral RNA and Infectious Virus Titers in Lung Tissues in a Syrian Hamster Model of Infection 39
2.2.4 MOV Inhibits Replication of SARS-CoV-2 Variants of Concern in a Syrian Hamster Model of Infection 39
2.2.5 SARS-CoV-1 and MERS-CoV 40
2.2.6 Influenza Virus 42
2.2.7 Venezuelan Equine Encephalitis Virus 43

[redacted]

C Confidential

2.2.8 Ebola Virus 43
3 SECONDARY PHARMACODYNAMICS 45
4 SAFETY PHARMACOLOGY 45
4.1 Neuropharmacological Profile (NPP) of Orally Administered MOV in Rats (TT #[redacted]-7812) 47
4.2 MOV: Effect on hERG Current (TT #[redacted]-7807) 47
4.3 NHC: Effect on Cloned hERG Potassium Channels Expressed in Human Embryonic Kidney Cells (TT #[redacted]-9400) 47
4.4 Evaluation of Cardiovascular Function Following Oral Administration of MOV in Conscious Telemetered Beagle Dogs (TT #[redacted]-7811) 48
4.5 MOV: Oral Cardiovascular Telemetry Study in Beagle Dogs (TT #[redacted]-5603) 48
4.6 Pulmonary Assessment of Orally Administered MOV in the Conscious Rat (TT #[redacted]-7813) 49
5 PHARMACODYNAMIC DRUG INTERACTIONS 50
5.1 Impact of Drug Combination on Antiviral Activity 50
6 DISCUSSION AND CONCLUSIONS 51
7 LIST OF REFERENCES 54

[redacted]

LIST OF TABLES

Table 2.6.2: 1 Nonclinical Pharmacologic Studies Supporting Development of MOV ... 10
Table 2.6.2: 2 NHC Antiviral Activity Against SARS-CoV-2, SARS-CoV, and MERS-CoV in Cell Lines and Primary Human Bronchial/Tracheal Epithelial Cells ... 17
Table 2.6.2: 3 NHC Antiviral Activity Against SARS-CoV-2 in Multiple Susceptible Cell Lines ... 18
Table 2.6.2: 4 NHC Antiviral Activity Against Influenza A and B Viruses in Cell Lines and Primary Human Bronchial/Tracheal Epithelial Cells ... 21
Table 2.6.2: 5 NHC Antiviral Activity Against Togaviruses in Cell Lines ... 22
Table 2.6.2: 6 NHC Antiviral Activity Against Ebola Virus in Vero Cells ... 22
Table 2.6.2: 7 NHC Antiviral Activity Against SARS-CoV-2 Variants of Concern in Vero E6 Cells ... 24
Table 2.6.2: 8 Molnupiravir and NHC Antiviral Activity Against SARS-CoV-2 Variants ... 25
Table 2.6.2: 9 NHC Antiviral Activity Against SARS-CoV-2 Variants Lambda and Mu in Vero E6 Cells ... 26
Table 2.6.2: 10 N-Hydroxycytidine Activity Against SARS-CoV-2 With Remdesivir Resistance-associated and MOV Treatment-emergent Amino Acid Substitutions in NSP12 (Polymerase) and NSP14 (Exonuclease) in the Reporter Replicon Assay ... 28
Table 2.6.2: 11 Cytotoxicity (CC_{50}) of NHC in Mammalian Cell Lines ... 33
Table 2.6.2: 12 Safety Pharmacology Studies with MOV (To Support ICH S7A and 7B Recommendations) ... 46
Table 2.6.2: 13 Evaluation of Drug Combination Impact on Antiviral Activity and Cytotoxicity in a SARS-CoV-2 Infection Assay ... 51

[redacted]

C Confidential

LIST OF FIGURES

Figure 2.6.2: 1 Inhibition of SARS-CoV-2 and MERS-CoV by NHC in Vero and Calu-3 Cell Lines 19
Figure 2.6.2: 2 Inhibition of SARS-CoV-2 by NHC in Human Airway Epithelial Cells 20
Figure 2.6.2: 3 Antiviral Activity of NHC Against SARS-CoV-2 Alpha (B.1.1.7), Beta (B.1.351), Gamma (P.1), and Delta (B.1.617.2) Variants of Concern 23
Figure 2.6.2: 4 Remdesivir-resistance Mutations in Coronavirus Increase Susceptibility to NHC 30
Figure 2.6.2: 5 Activity of MOV Against Remdesivir-resistant SARS-CoV-2 31
Figure 2.6.2: 6 Time Course Profile of Intracellular NHC-TP Concentrations After Treatment of Human, Dog, or Rat PBMCs With 0.2, 2, or 20 µM NHC 32
Figure 2.6.2: 7 Pre-exposure Prophylaxis and Post-exposure Treatment With MOV (EIDD-2801) Potently Prevents SARS-CoV-2 Infection In Vivo 35
Figure 2.6.2: 8 Therapeutic Oral Administration of MOV is Efficacious Against SARS-CoV-2 in a Ferret Infection Model 37
Figure 2.6.2: 9 Therapeutic Oral Administration of MOV Prevents Contact Transmission of SARS-CoV-2 in a Ferret Infection Model 38
Figure 2.6.2: 10 Syrian Hamster Model Study Design, Viral Shedding, Viral Load, Infectious Titers, and Viral Antigen 39
Figure 2.6.2: 11 MOV Reduces Viral Loads in Syrian Hamsters Infected With Different SARS-CoV-2 Variants 40
Figure 2.6.2: 12 Prophylactic and Therapeutic Treatment With MOV Reduces SARS-CoV Replication and Pathogenesis in Mice 42
Figure 2.6.2: 13 Antiviral Activity of MOV in the Ferret Model of Influenza (A/California/07/2009[H1N1]) 44

[redacted]

LIST OF ABBREVIATIONS, ACRONYMS AND DEFINITION OF TERMS

This list serves as the first use of an abbreviation, acronym, or term.

Abbreviation/Acronym	Definition
3TC	Lamivudine
A	Amino acid single letter code for alanine
Ac. No.	Accession number
ACE2	Angiotensin-converting enzyme 2
ALI	Acute lung injury
ALI	Air-liquid interface
ANOVA	Analysis of variance
ATS	American Thoracic Society
B.1-G	SARS-CoV-2 Wuhan isolate
B.1.1.529	SARS-CoV-2 Omicron variant
B.1.1.7	SARS-CoV-2 Alpha variant
B.1.351	SARS-CoV-2 Beta variant
B.1.617.2	SARS-CoV-2 Delta variant
B.1.621	SARS-CoV-2 Mu variant
BID	Twice daily
BP	Blood pressure
BT	Body temperature
C.37	SARS-CoV-2 Lambda variant
CA	California
CC_{50}	Half-maximal cytotoxicity concentration
CDC	(US) Centers for Disease Control and Prevention
cDNA	Complementary deoxyribonucleic acid
CHKV	Chikungunya virus
C_{max}	Observed maximum concentration
CNS	Central nervous system
CoV	Coronavirus
COX-2	Human cyclooxygenase 2
COVID-19	Infection caused by SARS-CoV-2; coronavirus disease 2019
CPE	Cytopathic effect
CRL	Charles River Laboratories
CTP	Cytosine triphosphate cytidine triphosphate
Ctrl	Control
d	Day(s)

[redacted]

Abbreviation/Acronym	Definition
D	Amino acid single letter code for aspartic acid
DAD	Diffuse alveolar damage
DBP	Diastolic blood pressure
DBT	Murine astrocytoma delayed brain tumor
Dept.	Department
DMSO	Dimethyl sulfoxide
DNA	Deoxyribonucleic acid
dNTP	Deoxynucleoside triphosphate
E	Amino acid single letter code for glutamic acid
EBOV	Ebola virus
EC_{50}	Half-maximal effective concentration
EC_{90}	90% effective concentration
ECG	Electrocardiogram
EEEV	Eastern equine encephalitis virus
EIDD	Emory Institute for Drug Development
EIDD-2801	MK-4482
F	Amino acid single letter code for phenylalanine
FTC	Emtricitabine
G	Guanosine
g	Gram(s)
GFP	Green fluorescent protein
GISAID	Global Initiative on Sharing All Influenza Data
GLP	Good Laboratory Practice
GMP	Good Manufacturing Practices
h, Hr	Hour
HAE	Human airway epithelium
HBEC	Human bronchial epithelial cell
HEK	Human embryonic kidney
hERG	Human ether-à go-go related gene
HR	Heart rate
I	Amino acid single letter code for isoleucine
IAV	Influenza A virus
IBV	Influenza B virus
IC_{50}	Half-maximal inhibitory concentration
ICH	International Council for Harmonisation of Technical Requirements for Pharmaceuticals for Human Use
ID	Identification

[redacted]

Abbreviation/Acronym	Definition
IKr	Rapidly activating delayed rectifier cardiac potassium current
L	Amino acid single letter code for leucine
LoD	Limit of detection
LoM	Lungs only mice
MBP	Mean blood presuure
MDCK	Madin-Darby Canine Kidney
MERS	Middle east respiratory syndrome
MERS-CoV	Middle east respiratory syndrome-associated coronavirus
MHV	Mouse hepatitis virus, a model coronavirus
MOI	Multiplicity of infection
MOV	Molnupiravir or MK-4482
MTFR	Median time to resolve fever
n, No.	Number
N/A, NA	Not applicable
ND	Not determined
NHC	EIDD-1931 or N-hydroxycytidine
NHC-DP	N-hydroxycytidine diphosphate
NHC-MP	N-hydroxycytidine monophosphate
NHC-TP	EIDD-2061 or the triphosphate of N-hydroxycytidine
[redacted]	[redacted]
nLUC	Nanoluciferase
NP	Nasopharyngeal
NPP	Neuropharmacological Profile
NSP	Nonstructural protein
OECD	Organisation for Economic Co-operation and Development
P	Amino acid single letter code for proline
P.1	SARS-CoV-2 Gamma variant
PBMC	Peripheral blood mononuclear cell
PenH	Enhanced pause
pfu	Plaque-forming unit(s)
pI, p.i.	Post-infection
POLRMT	Mitochondrial DNA-dependent RNA polymerase
Q12H	Every 12 hours
RdRp	RNA-dependent RNA polymerase
RNA	Ribonucleic acid
RSV	Respiratory syncytial virus

Abbreviation/Acronym	Definition
RT-PCR	Reverse transcriptase polymerase chain reaction
Rx	Treatment
S	Amino acid single letter code for serine
SARS	Severe acute respiratory syndrome
SARS-CoV-1	SARS-associated coronavirus-1
SARS-CoV-2	SARS-associated coronavirus-2
SBP	Systolic blood pressure
SD	Standard deviation
SEM	Standard error of the mean
SI	Selectivity index
SN	Study number
T	Amino acid single letter code for threonine
$TCID_{50}$	50% tissue culture infectious dose
US, USA	United States of America
[redacted]	[redacted]
UTP	Uridine 5′-triphosphate
V	Amino acid single letter code for valine
VEEV	Venezuelan equine encephalitis virus
WA1	SARS-CoV-2, Isolate USA-WA1/2020
WT	Wild-type
Y	Amino acid single letter code for tyrosine
ZIKV	Zika virus

[redacted]

C Confidential

1 BRIEF SUMMARY

Molnupiravir (MOV; MK-4482) is the 5′-isobutyrate prodrug of the broadly active, antiviral ribonucleoside analog N-hydroxycytidine (NHC) developed for the oral treatment of adult patients with COVID-19. MOV is hydrolyzed by esterases either during or after absorption to deliver NHC into systemic circulation. Once distributed inside cells, NHC is phosphorylated to its corresponding triphosphate anabolite (NHC-TP), and acts as a competitive alternative substrate for virally encoded RdRp. MOV and NHC inhibit replication of viral pathogens from multiple RNA virus families, including pathogenic coronavirus such as SARS-CoV-2. Antiviral activity has been verified in animal models of coronavirus virus infection.

MOV, an oral direct-acting antiviral agent, will address the critical need for different therapeutic agents to treat COVID-19. MOV is administered orally enabling patients to initiate therapy in an outpatient setting. This flexibility in outpatient management would help to limit direct patient interactions with health care staff and decrease transmission risk, which is significant due to the highly contagious nature of SARS-CoV-2. In vitro, NHC has a high genetic barrier to resistance and remains active against SARS-CoV-2 variants of concern.

Primary pharmacology studies demonstrating the antiviral activity of MOV against SARS-CoV-2 and other RNA viruses were conducted in vitro and in mouse, guinea pig, hamster, and ferret models of viral infection. In vitro, NHC shows broad-spectrum activity against multiple viruses including coronaviruses SARS-CoV-2, SARS-CoV, and MERS-CoV. NHC was equally effective against SARS-CoV-2 variants of concern B.1.1.7 (Alpha), B.1.351 (Beta), P.1 (Gamma), B.1.617.2 (Delta), B.1.1.529 (Omicron), and BA.1.1 (Omicron), variant of interest C.37 (Lambda), and variant being monitored B.1.621 (Mu) compared with the WA1 isolate. NHC was active against coronaviruses that have mutations which reduce susceptibility to remdesivir in cell culture assays. NHC was similarly active against replicons with remdesivir resistance-associated amino acid substitutions in NSP12 (polymerase) and MOV treatment-emergent NSP12 and NSP14 (exonuclease) variants in the reporter replicon assay.

NHC was efficiently taken up by cell lines, PBMCs, and HBEC air-liquid interface cultures, and phosphorylated to mono-, di-, and tri-phosphate forms. NHC was phosphorylated to NHC-TP in a dose-dependent manner in human, dog, and rat PBMCs. The phosphorylated forms of NHC are catabolized in a few hours in cell lines, HBEC air-liquid interface cultures, and PMBCs. NHC-TP is detectable at least 24 hours after treatment with 10 µM NHC in HBEC air-liquid interface cultures.

Antiviral activity of MOV was also demonstrated in animal infection models of SARS-CoV-2, MERS-CoV, and influenza. MOV (500 mg/kg) significantly reduced infectious SARS-CoV-2 levels in lung tissue from LoM when administered 12 hours prior, 24 hours post, or 48 hours post direct infection of human lung tissue, followed by twice daily dosing thereafter. In a ferret model, treatment with MOV reduced SARS-CoV-2 infectious viral titers in nasal secretions from infected ferrets and suppressed all viral transmission to the untreated direct contacts, despite prolonged direct proximity between source and contact animals. In a Syrian hamster model of SARS-CoV-2 infection and disease, MOV

prophylactic or therapeutic treatment showed decreased viral RNA titers and infectious virus from lungs several days postinfection. In a Syrian hamster model of SARS-CoV-2 infection and disease using either the B.1-G (Wuhan strain), B.1.1.7 (Alpha), or B.1.351 (Beta) variants of SARS-CoV-2, treatment with 200 mg/kg BID MOV resulted in statistically significant reductions in viral RNA copies in lungs and in infectious virus lung titers regardless of variant.

Prolonged in vitro exposure (14 days) of CEM and HepG2 cells with NHC did not result in mitochondrial toxicity or dysfunction. Neither MOV nor NHC exhibited off-target activities of clinical concern. NHC-TP had calculated IC_{50} values >1000 µM under physiological concentrations of dNTPs for human DNA polymerases α, β, and γ.

MOV was devoid of effects on CNS, respiratory, or cardiovascular functions in well-characterized safety pharmacology models. NHC C_{max} exposure margins were based on population pharmacokinetics analysis in adult patients with COVID-19 from P001 and P002 clinical trials (Part 1), where a 800 mg Q12H MOV dose resulted in systemic mean exposures C_{max} of 10.8 µM the NHC

There was no impact on the in vitro antiviral activity of NHC against SARS-CoV-2 in two-drug combination studies with 3TC, abacavir, FTC, hydroxychloroquine, nelfinavir, remdesivir, ribavirin, sofosbuvir, or tenofovir.

The nonclinical pharmacologic studies and literature references supporting MOV are shown in [Table 2.6.2: 1].

Table 2.6.2: 1 Nonclinical Pharmacologic Studies Supporting Development of MOV

Source or Report No.	Study Title	Test System / Species	Testing Facility / Literature Reference	GLP
Primary Pharmacodynamics – In Vitro				
Hernandez-Santiago et al, 2004; Painter et al, 2019; Flavell et al, 1974; Gordon et al, 2021; Kabinger et al, 2021; Mullins et al, 2011; Agostini et al, 2019; Toots et al, 2019; Urakova et al, 2018; Sheahan et al, 2020; Szemiel et al, 2021	Mechanism of action	In vitro	[Ref. 4.3: 05JF07], [Ref. 4.3: 05JM4T], [Ref. 4.3: 05JF06], [Ref. 4.3: 06G33J], [Ref. 4.3: 06G338], [Ref. 4.3: 05JF08], [Ref. 4.3: 05JF05], [Ref. 4.3: 05JF0D], [Ref. 4.3: 05JF0F], [Ref. 4.3: 05K8L0], [Ref. 4.3: 05R3M7]	No
Merck Report PD001 (EIDD Report 25.038)	Defining Efficacy and Cytotoxicity for SARS-CoV Infected Human Lung Cells Treated with EIDD-1931	In vitro	[redacted] USA	No

[redacted]

C Confidential

Table 2.6.2: 1 Nonclinical Pharmacologic Studies Supporting Development of MOV

Source or Report No.	Study Title	Test System / Species	Testing Facility / Literature Reference	GLP
Merck Report PD006	In Vitro Evaluation of One Test Compound (EIDD-2801) on Human Myeloid and Erythroid Colony Forming Cell Assays (EMY-05)	In vitro	[redacted] USA	No
Merck Report PD007	In Vitro Assessment of Antiviral Activity of MK-4482 and N-Hydroxycytidine in Multiple Susceptible Cell Lines	In vitro	Merck Research Laboratories[a] West Point, Pennsylvania, USA [redacted] USA [redacted] USA [redacted] USA [redacted] USA	No
Merck Report PD008	In Vitro Antiviral Activity of N-hydroxycytidine Against SARS-CoV-2 And Other Viruses	In vitro	Merck Research Laboratories[a] West Point, Pennsylvania, USA [redacted] USA	No
Merck Report PD009	In Vitro Cytotoxicity Evaluations of Compounds MK595 and MK596, [redacted], Study SE141853	In vitro	[redacted] USA	No
Merck Report PD010	Evaluation of N-Hydroxycytidine Antiviral Activity Against SARS-CoV-2 Variants in Vero Cells	In vitro	[redacted] USA Merck Research Laboratories[a] West Point, Pennsylvania, USA	No

Table 2.6.2: 1 Nonclinical Pharmacologic Studies Supporting Development of MOV

Source or Report No.	Study Title	Test System / Species	Testing Facility / Literature Reference	GLP
Merck Report PD011	Evaluation of Amino Acid Substitutions in SARS-CoV-2 NSP12 (Polymerase) and NSP14 (Exonuclease) on the Antiviral Activity of N-Hydroxycytidine in a Replicon Model	In vitro	Merck Research Laboratories[a] West Point, Pennsylvania, USA	No
Merck Report PD012	In Vitro Evaluation of NHC Uptake By Cell Lines, By Human, Dog, and Rat Peripheral Blood Mononuclear Cells, and In Human Bronchial Epithelial Cell (HBEC) Air-liquid Interface (ALI) Cultures	In vitro	Merck Research Laboratories[a] West Point, Pennsylvania, USA Merck Research Laboratories MRL Cambridge ESC Cambridge, Massachusetts, USA	No
Merck Report PD014	Evaluation of N-Hydroxycytidine Antiviral Activity Against SARS-CoV-2 Variants Lambda and Mu in Vero Cells	In vitro	[redacted] USA Merck Research Laboratories[a] West Point, Pennsylvania, USA	No
Merck Report PD015	Evaluation of N-Hydroxycytidine Antiviral Activity Against the SARS-CoV-2 Omicron Variant in Vero Cells	In vitro	[redacted] USA Merck Research Laboratories[a] West Point, Pennsylvania, USA	No
[redacted]	Antiviral activity in cell lines and human airway epithelium	In vitro	[Ref. 4.3: 06FR0T]	No
Sheahan et al, 2020			[Ref. 4.3: 05K8L0]	
Agostini et al., 2019			[Ref. 4.3: 05JF05]	
Toots et al., 2019			[Ref. 4.3: 05JF0D]	
Urakova 2018			[Ref. 4.3: 05JF0F]	
Sheahan et al, 2020	Antiviral activity against coronavirus resistant to remdesivir	In vitro	[Ref. 4.3: 05K8L0]	No
Szemiel et al, 2021			[Ref. 4.3: 05R3M7]	

[redacted]

C Confidential

Table 2.6.2: 1 Nonclinical Pharmacologic Studies Supporting Development of MOV

Source or Report No.	Study Title	Test System / Species	Testing Facility / Literature Reference	GLP
[redacted]; Yoon et al, 2018; Toots et al, 2019	Antiviral activity against Influenza A and B viruses	In vitro	[Ref. 4.3: 06FR0T], [Ref. 4.3: 05JF0G], [Ref. 4.3: 05JF0D]	No
[redacted]; Urakova et al, 2018	Antiviral activity against togaviruses	In vitro	[Ref. 4.3: 06FR0T], [Ref. 4.3: 05JF0F]	No
[redacted]	Antiviral activity against Ebola virus	In vitro	[Ref. 4.3: 06FR0T]	No
Reynard et al, 2015; erratum, 2016			[Ref. 4.3: 06CK43]	
Sticher et al, 2020; Yoon et al, 2018	Cytotoxicity in tissue culture utilizing cells from different organs and species	In vitro	[Ref. 4.3: 05JF0B], [Ref. 4.3: 05JF0G]	No
Sticher et al, 2020	Assessment of mitochondrial toxicity	In vitro	[Ref. 4.3: 05JF0B]	No
Primary Pharmacodynamics – In Vivo				
Wahl et al, 2021	Activity in a pre-exposure prophylaxis lung only mouse model of SARS-CoV-2 coronavirus infection	SARS-CoV-2: Human Lung-only Mouse	[Ref. 4.3: 05R3M8]	No
Cox et al, 2020	Activity and prevention of contact transmission in a ferret model of SARS-CoV-2 coronavirus infection	SARS-CoV-2: Ferret	[Ref. 4.3: 05NRF7]	No
Rosenke et al, 2021	Activity in a Syrian hamster model of SARS-CoV-2 coronavirus infection	SARS-CoV-2: Syrian hamster	[Ref. 4.3: 05R3LW]	No
Abdelnabi et al, 2021	Activity in a Syrian hamster model of SARS-CoV-2 coronavirus infection against variants of concern	SARS-CoV-2: Syrian hamster	[Ref. 4.3: 06FGX5]	No
Sheahan et al, 2020	Activity in models of coronavirus infection	SARS-CoV-1: C57BL/6 Mouse MERS-CoV: hDPP4 288/330 Mouse	[Ref. 4.3: 05K8L0]	No
Toots et al, 2019; Toots et al, 2020	Activity in models of influenza virus infection	Ferret	[Ref. 4.3: 05JF0D], [Ref. 4.3: 05JF09]	No

[redacted]

C Confidential

Table 2.6.2: 1 Nonclinical Pharmacologic Studies Supporting Development of MOV

Source or Report No.	Study Title	Test System / Species	Testing Facility / Literature Reference	GLP
Painter et al, 2019	Activity in models of Venezuelan equine encephalitis virus infection	Mouse	[Ref. 4.3: 05JM4T]	No
Merck Report PD002 (STDY-16-0019-JC)	Efficacy of Orally Administered EIDD-01931 in the Intraperitoneal Ebolavirus Challenge BALB/c Mouse Model – Study 3	Mouse	USA	No
Secondary Pharmacodynamics				
Merck Report PD003 SN: EMO022216-1	Data Report, Report No. EMO022216-1	In vitro	USA	No
Merck Report PD004	Assessment of the Off-target Activity of MK-4482 and N-hydroxycytidine in a Panel of Enzyme, Radioligand Binding, and Functional Assays	In vitro	Merck Research Laboratories[a] West Point, Pennsylvania, USA Taiwan	No
Merck Report PD013	Determination of the Effect of N-Hydroxycytidine Triphosphate on the Activity of Human DNA Polymerases Alpha, Beta, and Gamma	In vitro	Merck Research Laboratories[a] Kenilworth, New Jersey, USA	No
Safety Pharmacology				
TT # -7812	Neuropharmacological Profile (NPP) of Orally Administered EIDD-2801 in Rats	Rat	USA	Yes
TT # -7807	Effect of EIDD-2801on Cloned hERG Potassium Channels Expressed in Human Embryonic Kidney Cells	In vitro: HEK cells	Canada	Yes [b]
TT # -9400	Effect of N-Hydroxy Cytidine on Cloned hERG Potassium Channels Expressed in Human Embryonic Kidney Cells	In vitro: HEK cells	USA	Yes [c]

Table 2.6.2: 1 Nonclinical Pharmacologic Studies Supporting Development of MOV

Source or Report No.	Study Title	Test System / Species	Testing Facility / Literature Reference	GLP
TT # -7811	Evaluation of Cardiovascular Function Following Oral Administration of EIDD-2801 in Conscious Telemetered Beagle Dogs	Beagle dogs	USA	Yes
TT # -5603 Merck Research Laboratories	Oral Cardiovascular Telemetry Study in Beagle Dogs	Beagle dogs	Merck Research Laboratories[a] West Point, Pennsylvania, USA	Yes
TT # -7813	Pulmonary Assessment of Orally Administered EIDD-2801 in the Conscious Rat	Rat	USA	Yes
Pharmacodynamic Drug Interactions				
Merck Report PD005	In Vitro Assessment of Antiviral Activity of N-hydroxycytidine and the Impact of Two-drug Combinations	In vitro	Merck Research Laboratories[a] West Point, Pennsylvania, USA USA	No

ALI=air-liquid interface; = ; = ; Dept.=department; EIDD=Emory Institute for Drug Development; EIDD-2801=molnupiravir or MK-4482; GLP=Good Laboratory Practice; = ; HBEC=human bronchial epithelial cell; hERG=human ether-à-go-go-related gene; = (USA); No.=number; MERS-CoV=Middle east respiratory syndrome-associated coronavirus; NPP=neuropharmacological profile; SARS-CoV=severe acute respiratory syndrome-associated coronavirus; SN=Study number; USA=United States of America; = .

[a] Merck Research Laboratories is a division of Merck, Sharp & Dohme Corp. (MSD).

[b] MOV hERG (TT # -7807): GLP

[c] NHC hERG (TT # -9400): GLP

2 PRIMARY PHARMACODYNAMICS

2.1 In Vitro Pharmacology

2.1.1 Mechanism of Action

The prodrug, MOV, is hydrolyzed by esterases to NHC, which circulates systemically and is taken up by cells. Intracellular kinases phosphorylate NHC to its corresponding active triphosphate, NHC-TP (Hernandez-Santiago et al, 2004; Painter et al, 2019) [Ref. 4.3: 05JF07], [Ref. 4.3: 05JM4T]. NHC-TP acts as a competitive alternative substrate to natural ribonucleotides for virally encoded RdRps and NHC 5′-monophosphate is incorporated into nascent viral RNA. Because the N^4-hydroxycytosine base of NHC can

tautomerize, NHC-TP can pair with either guanosine or adenosine, and then substitute for either CTP or UTP, respectively (Flavell et al, 1974; Gordon et al, 2021; Kabinger et al, 2021) [Ref. 4.3: 05JF06], [Ref. 4.3: 06G33J], [Ref. 4.3: 06G338]. This results in an accumulation of mutations in the viral genome with each cycle during viral replication. The process whereby the mutation rate is increased by exposure to a drug is referred to as Viral Decay Acceleration (Mullins et al, 2011) [Ref. 4.3: 05JF08] and results in viral ablation due to the mechanism of error catastrophe.

The error catastrophe mechanism of action for NHC, has been validated for MERS-CoV, VEEV, and IAV. Multi-log decreases in virus yields and significantly increased levels of RNA mutations were observed when viruses were propagated in the presence of NHC (Agostini et al, 2019; Toots et al, 2019; Urakova et al, 2018) [Ref. 4.3: 05JF05], [Ref. 4.3: 05JF0D], [Ref. 4.3: 05JF0F]. For VEEV, the infectivity of virions formed in the presence of NHC decreases (Urakova et al, 2018) [Ref. 4.3: 05JF0F]. This same effect, i.e., decrease in infectious virions, was demonstrated for coronaviruses (MERS-CoV, MHV; Agostini et al, 2019; see [Sec. 2.6.2: 2.1.2] for details) [Ref. 4.3: 05JF05] and influenza viruses A and B (Toots et al, 2019) [Ref. 4.3: 05JF0D]. NHC was also shown to be active against coronavirus resistant to remdesivir in cell culture assays (Sheahan et al, 2020; Szemiel et al, 2021; [Sec. 2.6.2: 2.1.5.2]) [Ref. 4.3: 05K8L0], [Ref. 4.3: 05R3M7].

2.1.2 Antiviral Activity of NHC In Vitro

NHC has demonstrated specific, dose-dependent inhibition of viral replication with sub- to low-micromolar EC_{50} values against SARS-CoV-2 ([Table 2.6.2: 2], [Table 2.6.2: 3], [Figure 2.6.2: 1], and [Figure 2.6.2: 2]), SARS-CoV-1 [Table 2.6.2: 2], and MERS-CoV [Table 2.6.2: 2], in multiple cell types, including Vero E6, Huh-7, Calu-3 lung epithelial cells, and A549-ACE2 cells. The antiviral activity of NHC did not correlate with cellular cytotoxicity concentrations as observed CC_{50} values were generally greater than the highest concentration evaluated (i.e. SI values >4 in most studies). The EC_{50} values of MOV for antiviral activity were higher than those of NHC (Nonclinical Study Report PD007) [Sec. 2.6.3: 1].

NHC shows specific antiviral activity for all influenza viral isolates tested in different tissue culture cell lines and in the differentiated organoid model of human airway epithelium with a selectivity index of ≥21. It is active against influenza A (pandemic and seasonal) and influenza B strains, as well as against highly pathogenic H5N1 and H7N9 strains [Table 2.6.2: 4].

NHC also showed antiviral activity against togaviruses (genus alphavirus) VEEV, EEEV, and CHKV [Table 2.6.2: 5], and against Ebola virus [Table 2.6.2: 6].

Table 2.6.2: 2 NHC Antiviral Activity Against SARS-CoV-2, SARS-CoV, and MERS-CoV in Cell Lines and Primary Human Bronchial/Tracheal Epithelial Cells

Virus	Strain	Cell line	EC_{50} (µM)	CC_{50} (µM)	SI	Source/Reference
SARS-CoV-2	2019-nCoV/USA-WA1/2020; GenBank Ac. No. MN985325.1	Calu-3 2B4[a]	0.08	>10	>125	Sheahan et al, 2020 [Ref. 4.3: 05K8L0]
		Vero E6	0.30	>10	>33	
SARS-CoV-1	Urbani	Vero76	<0.4	144	>360	[redacted] [Ref. 4.3: 06FR0T]
SARS-CoV-1	SARS-CoV-GFP[b]	HAE-3D[c]	<1	>100	>100	PD001 (EIDD Report 25.038) [Sec. 2.6.3: 1]
SARS-CoV-1	SARS-CoV-GFP[b]	HAE	0.14	>100	>714	Sheahan et al, 2020 [Ref. 4.3: 05K8L0]
MERS-CoV	MERS-nLUC[d]	Calu-3 2B4[a]	0.15	>10	>67	Sheahan et al, 2020 [Ref. 4.3: 05K8L0]
MERS-CoV	GenBank Ac. No. JX869059[e]	DBT-9	0.56	>200	>357	Agostini et al, 2019 [Ref. 4.3: 05JF05]
MERS-CoV	Human β-CoV[e], Lineage C Novel 2012	Vero E6	<0.8	20	>25	[redacted] [Ref. 4.3: 06FR0T]

Ac. No.=Accession Number; CC_{50}=half-maximal cytotoxicity concentration; cDNA=complementary DNA; DBT=murine astrocytoma delayed brain tumor; EC_{50}=half-maximal effective concentration; GFP=green fluorescent protein; HAE=human airway epithelium; MERS-CoV=Middle east respiratory syndrome-associated coronavirus; NHC=EIDD-1931 or N-hydroxycytidine; [redacted] (USA); nLUC=nanoluciferase; SARS-CoV-1=Severe acute respiratory syndrome-associated coronavirus-1; SI=selectivity index.

[a] Calu-3 2B4 is a human lung epithelial cell line.

[b] SARS-CoV engineered to express green fluorescent protein

[c] HAE organoid model.

[d] MERS-nLUC is a recombinant MERS-CoV engineered to express nanoluciferase.

[e] cDNA-derived clone.

[redacted]

C Confidential

Table 2.6.2: 3 NHC Antiviral Activity Against SARS-CoV-2 in Multiple Susceptible Cell Lines

Laboratory	Cell Line	EC_{50} (µM)	CC_{50} (µM)	SI
[redacted]	Vero E6 [a]	1.44	>30	>20.8
		2.03	>30	>14.8
		1.23	>30	>24.4
		0.97	>20	>20.6
[redacted]	Huh-7 [b]	2.08	>40.34	>19.4
		2.25	>40.34	>17.9
[redacted]	A549-ACE2 [c]	0.691	ND	ND
		0.672	ND	ND
[redacted]	A549-ACE2 [d]	2.66	>36	>15.5
		2.03	>36	>17.7
		2.16	>10	>4.62
		28.98 [f]	>36	>1.24
		1.44	>36	>25.0
[redacted]	VeroE6-TMPRSS2 [e]	0.32	ND	ND
		0.94	4.62	4.91
		1.08 [f]	19.3	17.9
		1.14	>10	>8.77
		0.49	4.39	8.96
[redacted]	Vero E6 [g]	0.78	>100	>130

ACE2=angiotensin-converting enzyme 2; CC_{50}=half-maximal cytotoxicity concentration; EC_{50}=half-maximal effective concentration; [redacted] = [redacted]; µM=micromolar; ND = not determined; NHC=EIDD-1931 or N-hydroxycytidine; SARS-CoV-2=severe acute respiratory syndrome associated-coronavirus-2; SI=selectivity index; TMPRSS2=transmembrane protease serine 2; [redacted] = [redacted].

[a] The [redacted] assay used Vero E6 cells and the SARS-CoV-2 USA_WA1/2020 strain virus.

[b] The [redacted] assay used Huh-7 cells and the hCoV-229E virus.

[c] The [redacted] assay used A549-ACE2 cells and an N-luciferase-derived SARS-CoV-2 USA_WA1/2020 strain virus.

[d] This [redacted] assay used A549-ACE2 cells and mNeonGreen SARS-CoV-2 (icSARS-CoV-2-mNG), a reverse genetic variant of 2019-nCoV/USA_WA1/2020.

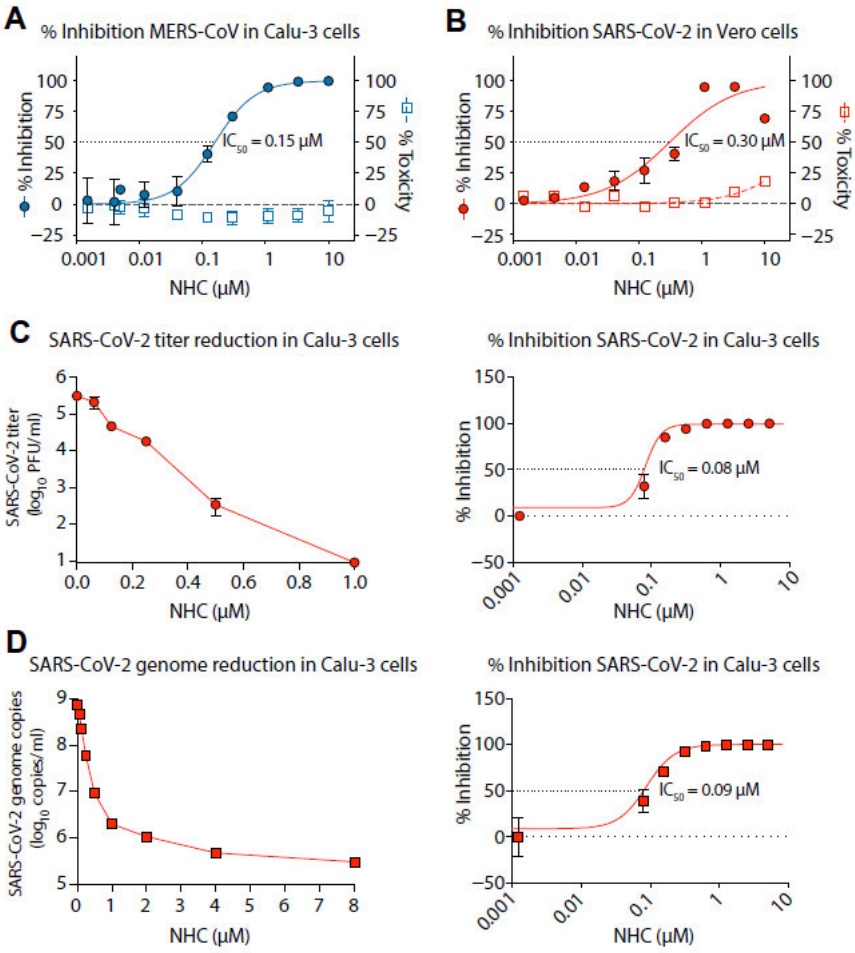
[e] This [redacted] assays used VeroE6-TMPRSS2 cells and mNeonGreen SARS-CoV-2 (icSARS-CoV-2-mNG), a reverse genetic variant of 2019-nCoV/USA_WA1/2020.

[f] This assay was performed using a 384-well format.

[g] The [redacted] assay used Vero E6 cells and SARS-CoV-2 USA-WA1/2020.

Source: Adapted from Nonclinical Study Reports PD007, and PD008 [Sec. 2.6.3: 1].

Figure 2.6.2: 1 Inhibition of SARS-CoV-2 and MERS-CoV by NHC in Vero and Calu-3 Cell Lines



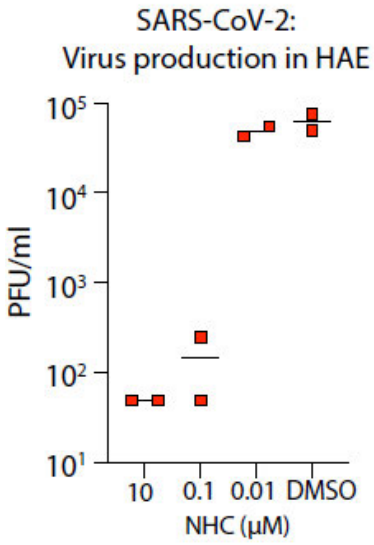
hr=hour; IC_{50}=half-maximal inhibitory concentration; MERS-CoV=Middle east respiratory syndrome-associated coronavirus; MOI=multiplicity of infection; NHC=EIDD-1931 or N-hydroxycytidine; pfu=plaque-forming unit(s); RNA=ribonucleic acid; SARS-CoV-2=Severe acute respiratory syndrome-associated coronavirus 2.

NHC antiviral activity (closed circles) and cytotoxicity (open squares) against MERS-CoV and SARS-CoV-2 in Vero and Calu-3 cells. Cell viability was measured by CellTiter-Glo assay. **Panel** A: Percent inhibition of MERS-CoV replication and toxicity in Calu-3 cells after infection in triplicate with MERS-CoV nanoluciferase at a MOI of 0.08 in the presence of drug for 48 hrs, after which replication was quantified by luciferase expression. **Panel B**: Vero cells were infected in duplicate with SARS-CoV-2 clinical isolate virus (2019-nCoV/USA-WA1/2020) at an MOI of 0.05 in the presence of a dose response of NHC for 48 hrs after which replication was measured through quantitation of cell viability by CellTiter-Glo assay; cytotoxicity was measure in similarly treated by uninfected cultures. **Panel C:** SARS-CoV-2 titer reduction (left) and percent inhibition (right) in Calu-3 cells after infection at a MOI of 0.1 for 30 minutes (n=3), and then incubation with NHC for 72 hrs. Virus titer was measured by plaque assay. **Panel D:** SARS-CoV-2 genomic RNA reduction (left) and percent inhibition (right) in Calu-3 cell, where viral RNA was isolated from clarified supernatants from the study in Panel C. Genome copy numbers was quantified using reverse transcriptase polymerase chain reaction. In all panels, the symbol represents the mean and error bars represent standard deviation.

Source: Adapted from Sheahan et al, 2020, Figure 1 [Ref. 4.3: 05K8L0].

[redacted]

Figure 2.6.2: 2 Inhibition of SARS-CoV-2 by NHC in Human Airway Epithelial Cells



DMSO=dimethyl sulfoxide; HAE=human airway epithelia; hr=hour; MOI=multiplicity of infection; NHC=EIDD-1931 or N-hydroxycytidine; pfu=plaque-forming unit(s); SARS-CoV-2=Severe acute respiratory syndrome-associated coronavirus 2.

Human airway epithelia cultures were infected at a MOI of 0.5 with clinical isolate SARS-CoV-2 for 2 hours in the presence of NHC in duplicate, after which virus was removed, cultures washed, and incubated with NHC for 48 hours. Apical washes were then collected for virus titration by plaque assay. The line represents the mean and each symbol represents titer from a single well. DMSO was included as a negative control.

Source: Adapted from Sheahan et al, 2020, Figure 2, panel A [Ref. 4.3: 05K8L0].

Table 2.6.2: 4 NHC Antiviral Activity Against Influenza A and B Viruses in Cell Lines and Primary Human Bronchial/Tracheal Epithelial Cells

Virus	Strain	Cell line	EC_{50} (µM)	CC_{50} (µM)	SI	Source/Reference
IAV H1N1	Ca/07/2009	MDCK	1.24	68	55	[redacted] [Ref. 4.3: 06FR0T]
IAV H1N1	WSN/33	MDCK	1.1	299.8	275	Yoon et al., 2018 [Ref. 4.3: 05JF0G]
IAV H1N1	WSN/33	primary hBTEC	5.4	-	-	Yoon et al., 2018 [Ref. 4.3: 05JF0G]
IAV H3N2	Perth/16/2009	MDCK	0.88	52	59	[redacted] [Ref. 4.3: 06FR0T]
IAV H3N2	Ohio/sw-10-132/2010	MDCK	3.2	299.8	94	Yoon et al., 2018 [Ref. 4.3: 05JF0G]
IAV H5N1	Duck/MN/1525/81	MDCK	1.28	27	21	[redacted] [Ref. 4.3: 06FR0T]
IAV H5N1	Vietnam/1203/2004	MDCK	0.14	299.8	2143	Yoon et al., 2018 [Ref. 4.3: 05JF0G]
IAV H7N9	Anhui/1/2013	MDCK	0.13	299.8	2308	Yoon et al., 2018 [Ref. 4.3: 05JF0G]
IBV	Florida/4/2006	MDCK	<0.4	76	>190	[redacted] [Ref. 4.3: 06FR0T]
IBV	Brisbane/60/08	MDCK	0.006	299.8	50000	Yoon et al., 2018 [Ref. 4.3: 05JF0G]
IAV H1N1	Ca/07/2009	HAE-3D [a]	0.08	137	1713	Toots et al., 2019 [Ref. 4.3: 05JF0D]
IAV H3N2	Wisconsin/67/2005	HAE-3D [a]	0.08	137	1713	Toots et al., 2019 [Ref. 4.3: 05JF0D]
IBV	Brisbane/60/08	HAE-3D [a]	0.06	137	2283	Toots et al., 2019 [Ref. 4.3: 05JF0D]

CC_{50}=half-maximal cytotoxicity concentration; EC_{50}=half-maximal effective concentration; HAE=human airway epithelium; IAV H1N1=Influenza A virus H1N1; IBV=Influenza B virus; MDCK=Madin-Darby Canine Kidney; NHC=EIDD-1931 or N-hydroxycytidine; [redacted] = [redacted] (USA); SI=selectivity index.

[a] HAE organoid model.

[redacted]

C Confidential

Table 2.6.2: 5 NHC Antiviral Activity Against Togaviruses in Cell Lines

Virus	Strain	Cell line	EC_{50} (µM)	CC_{50} (µM)	SI	Source/Reference
VEEV	TC-83	Vero	0.43 [a]	>200	>465	Urakova 2018 [Ref. 4.3: 05JF0F]
VEEV	TC-83	Vero76	1.92	32	17	[redacted] [Ref. 4.3: 06FR0T]
EEEV	FL93-939	Vero76	1.08	84	78	[redacted] [Ref. 4.3: 06FR0T]
CHKV	S27 (VR-64)	Vero76	1.8	96	53	[redacted] [Ref. 4.3: 06FR0T]

CC_{50}=half-maximal cytotoxicity concentration; CHKV=chikungunya virus; EC_{50}=half-maximal effective concentration; EEEV=Eastern equine encephalitis virus; MOI=multiplicity of infection; [redacted] (USA); NHC=EIDD-1931 or N-hydroxycytidine; pfu=plaque-forming unit(s); SI=selectivity index; VEEV=Venezuelan equine encephalitis virus.

[a] MOI=20 pfu/cell; 24 hours post-infection.

Table 2.6.2: 6 NHC Antiviral Activity Against Ebola Virus in Vero Cells

Virus	Strain	Cell line	EC_{50} (µM)	CC_{50} (µM)	SI	Source/Reference
EBOV	Zaire	Vero	4.7	>100	>21	[redacted] [Ref. 4.3: 06FR0T]

CC_{50}=half-maximal cytotoxicity concentration; EBOV=Ebola virus; EC_{50}=half-maximal effective concentration; [redacted] (USA); NHC=EIDD-1931 or N-hydroxycytidine; SI=selectivity index.

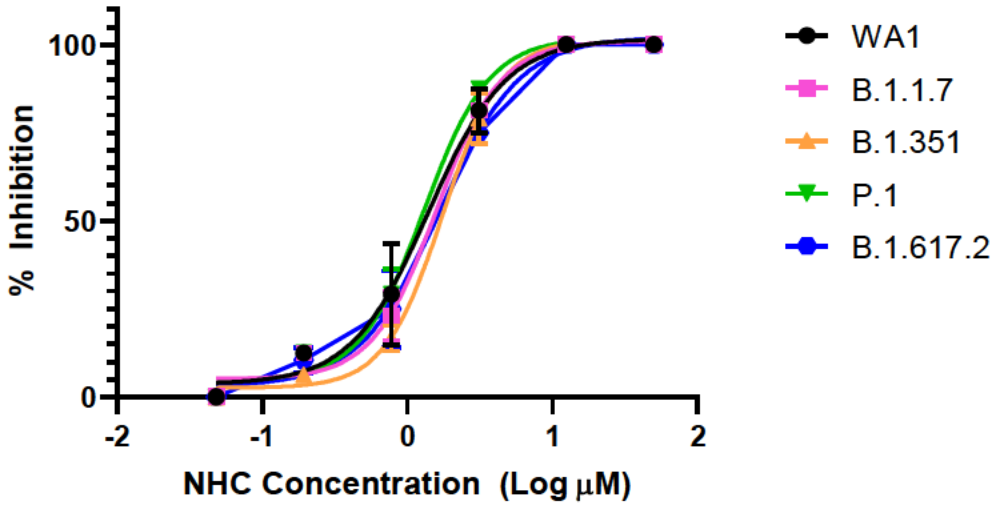
2.1.3 In Vitro Antiviral Activity of NHC Against SARS-CoV-2 Variants of Concern and Variants of Interest

The in vitro antiviral activity of NHC against SARS-CoV-2 variants of concern B.1.1.7 (Alpha), B.1.351 (Beta), P.1 (Gamma), and B.1.617.2 (Delta) was demonstrated at [redacted] USA) (Nonclinical Study Report PD010) [Sec. 2.6.3: 1]. The antiviral activity of NHC and remdesivir (control) were compared with the original WA1 (USA-WA1/2020) isolate using a cytopathic effect protection assay in Vero E6 cells (Iketani et al, 2021; Liu et al, 2020) [Ref. 4.3: 06FRN8] [Ref. 4.3: 06FRNB]. NHC antiviral activity was also assessed against SARS-CoV-2 variant of concern B.1.1.529 (Omicron) and BA.1.1 (Omicron) (Nonclinical Study Report PD015) [Sec. 2.6.3: 1], variant of interest C.37 (Lambda) and variant being monitored B.1.621 (Mu) (Nonclinical Study Report PD014) [Sec. 2.6.3: 1].

NHC inhibited SARS-CoV-2 variants B.1.1.7 (Alpha), B.1.351 (Beta), and P.1 (Gamma) with IC_{50} values of 1.59 µM, 1.77 µM, and 1.32 µM. respectively, compared with 1.41 µM for WA1 [Figure 2.6.2: 3], [Table 2.6.2: 7]. The corresponding IC_{50} values for remdesivir were 0.91 µM, 0.96 µM, and 0.59 µM and 1.07 µM for WA1 [Table 2.6.2: 7]. NHC inhibited

the SARS-CoV-2 variant B.1.617.2 (Delta) with an IC_{50} of 1.68 µM; the IC_{50} value for remdesivir was 1.08 µM [Figure 2.6.2: 3], [Table 2.6.2: 7].

Figure 2.6.2: 3 Antiviral Activity of NHC Against SARS-CoV-2 Alpha (B.1.1.7), Beta (B.1.351), Gamma (P.1), and Delta (B.1.617.2) Variants of Concern



B.1.1.7 = SARS-CoV-2 Alpha variant or SARS-CoV-2 Isolate hCoV-19/USA/CA_CDC_5574/2020; B.1.351 = SARS-CoV-2 Beta variant or SARS-CoV-2 hCoV-19/South Africa/KRISP-EC-K005321/2020; B.1.617.2 = SARS-CoV-2 Delta variant or SARS-CoV-2 Isolate hCoV-19/USA/PHC658/2021; CA = California; CDC = (US) Centers for Disease Control and Prevention; CPE = cytopathic effect; µM = micromolar; NHC = N-hydroxycytidine; P.1 = SARS-CoV-2 Gamma variant or SARS-CoV-2, hCoV-19/Japan/TY7-501/2021; SARS-CoV-2 = severe acute respiratory syndrome-associated coronavirus 2; SEM = standard error of the mean; USA = United States of America; WA1 = SARS-CoV-2, Isolate USA-WA1/2020.

Data points represent the mean ± SEM percent inhibition of viral CPE by NHC against each SARS-CoV-2 virus variant tested. The SARS-CoV-2 variants B.1.1.7 (Alpha), B.1.351 (Beta), and P.1 (Gamma) were evaluated at the same time while the B.1.617.2 (Delta) variant was assessed separately.

Source: Nonclinical Study Report PD010 [Sec. 2.6.3: 1].

[redacted]

Table 2.6.2: 7 NHC Antiviral Activity Against SARS-CoV-2 Variants of Concern in Vero E6 Cells

Compound	IC_{50} (µM)				
	WA1 (USA)	Delta B.1.617.2	Alpha B.1.1.7	Beta B.1.351	Gamma P.1
NHC	1.41	1.68	1.59	1.77	1.32
Remdesivir	1.07	1.08	0.91	0.96	0.59

B.1.1.7 = SARS-CoV-2 Alpha variant or SARS-CoV-2 Isolate hCoV-19/USA/CA_CDC_5574/2020; B.1.351 = SARS-CoV-2 Beta variant or SARS-CoV-2 hCoV-19/South Africa/KRISP-EC-K005321/2020; B.1.617.2 = SARS-CoV-2 Delta variant or SARS-CoV-2 Isolate hCoV-19/USA/PHC658/2021; CA = California; CDC = (US) Centers for Disease Control and Prevention; IC_{50} = half-maximal inhibitory concentration; µM = micromolar; NHC = N-hydroxycytidine; P.1 = SARS-CoV-2 Gamma variant or SARS-CoV-2, hCoV-19/Japan/TY7-501/2021; SARS-CoV-2 = severe acute respiratory syndrome-associated coronavirus 2; USA = United States of America; WA1 = SARS-CoV-2, Isolate USA-WA1/2020.

IC_{50} values were calculated from a four-parameter dose–response curve in GraphPad Prism 8.0. The dose-response data for NHC are shown in [Figure 2.6.2: 3].

Source: Nonclinical Study Report PD010 [Sec. 2.6.3: 1].

In two separate experiments, NHC had IC_{50} values of 1.06 µM and 1.12 µM for the SARS-CoV-2 omicron (B.1.1.529) variant and 3.35 µM and 1.86 µM for the omicron BA.1.1 variant [Table 2.6.2: 8]. These values are similar to those reported for SARS-CoV-2 WA1 and other SARS-CoV-2 variants such as B.1.1.7 (Alpha), B.1.351 (Beta), P.1 (Gamma), B.1.617.2 (Delta), C.37 (Lambda). and B.1.621 (Mu) (Nonclinical Study Reports PD010 and PD014) [Sec. 2.6.3: 1], and in line with published studies evaluating MOV or NHC against SARS-CoV-2 omicron and other variants (Bojkova et al, 2022; Dabrowska et al, 2021; Li et al, 2022; Rosales et al, 2022; Takashita et al, 2022; Vangeel et al, 2022) [Ref. 4.3: 07YNGB, 07YGG0, 07YKW6, 07YJSK, 07YNH8, 07YNFR].

Table 2.6.2: 8 Molnupiravir and NHC Antiviral Activity Against SARS-CoV-2 Variants

Study	Cell Type	SARS-CoV-2 Variant	Molnupiravir EC_{50} (µM)	NHC EC_{50} (µM)
MSD Nonclinical Study Report PD015	Vero E6	WT	ND	0.63
				1.10
		Omicron BA.1[a] (B.1.1.529)	ND	1.06
				1.12
		Omicron BA.1.1[a]	ND	3.35
				1.86
Vangeel et al, 2022 [Ref. 4.3: 07YNFR]	Vero E6-GFP	Alpha	3.6	2.3
		Omicron	1.9	ND
Bojkova et al, 2022 [Ref. 4.3: 07YNGB]	Caco-2	Delta	ND	0.81
		Omicron-1[b]	ND	3.87
		Omicron-2[b]	ND	2.85
	Calu-3	Delta	ND	0.40
		Omicron-1[b]	ND	0.94
		Omicron-2[b]	ND	0.71
Dabrowska et al, 2021 [Ref. 4.3: 07YGG0]	A549 (ACE2/TMPRSS2)	Delta	1.3	0.17
		Omicron	0.23	0.07
Rosales et al, 2022 [Ref. 4.3: 07YJSK]	HeLa	Delta	ND	12.8
		Omicron	ND	10.4
	Vero E6/ TMPRSS2	Delta	ND	1.81
		Omicron	ND	0.25
Takashita et al, 2022 [Ref. 4.3: 07YNH8]	Vero E6/ TMPRSS2	Delta	ND	0.83
		Omicron (B.1.1.529)	ND	0.43
Li et al, 2022 [Ref. 4.3: 07YKW6]	Calu-3	WT	1.97	ND
		Omicron	0.76	ND

ACE2=angiotensin-converting enzyme 2; B.1.1.529=SARS-CoV-2 omicron variant; EC_{50}=half-maximal effective concentration; GFP=green fluorescent protein; GISAID=Global Initiative on Sharing All Influenza Data; ID=identification; MSD=Merck, Sharp & Dohme Corp.; ND=not determined; NHC=N-hydroxycytidine; SARS-CoV-2=severe acute respiratory syndrome-associated coronavirus-2; TMPRSS2=transmembrane protease serine 2; USA=United States of America; WT=wild-type.

[a] MSD Nonclinical Study Report PD015 describing study performed by [redacted] USA. Two separate experiments were performed in Vero E6 cells using omicron B.1.1.529 GISAID ID EPI_ISL_7171744 and omicron BA.1.1 GISAID ID EPI_ISL_8690072.

[b] SARS-CoV-2 Omicron (B.1.1.529) isolates Omicron 1 = FFM-SIM0550/2021, GISAID ID EPI_ISL_6959871, GenBank ID OL800702; and Omicron 2 = FFM-ZAF0396/2021, GISAID ID EPI_ISL_6959868, GenBank ID OL800703).

Source: Adapted from Nonclinical Study Report PD015 [Sec. 2.6.3: 1].

[redacted]

C Confidential

NHC had IC_{50} values of 0.92 µM and 0.98 µM for SARS-CoV-2 variant C.37 (Lambda), and 1.05 µM and 1.94 µM for SARS-CoV-2 variant B.1.621 (Mu) compared to the historical IC_{50} value of 1.41 µM for WA1 [Table 2.6.2: 9].

The data show that NHC was similarly effective against SARS-CoV-2 variants of concern B.1.1.7 (Alpha), B.1.351 (Beta), P.1 (Gamma), B.1.617.2 (Delta), B.1.1.529 (Omicron) and BA.1.1 (Omicron), variant of interest C.37 (Lambda), and variant being monitored B.1.621 (Mu) compared with the WA1 isolate.

Table 2.6.2: 9 NHC Antiviral Activity Against SARS-CoV-2 Variants Lambda and Mu in Vero E6 Cells

Compound	IC_{50} (µM)				
		Lambda C.37		Mu B.1.621	
	WA1 (USA)	Assay 1	Assay 2	Assay 1	Assay 2
NHC	1.41	0.92	0.98	1.05	1.94

B.1.621=SARS-CoV-2 Mu variant or SARS-CoV-2 Isolate hCoV-19/USA/WI-UW-4340/2021; C.37=SARS-CoV-2 Lambda variant or SARS-Related Coronavirus 2 Isolate hCoV-19/Peru/un-CDC-2-4069945/2021; CDC=(US) Centers for Disease Control and Prevention; IC_{50}=half-maximal inhibitory concentration; NHC=N-hydroxycytidine; SARS-CoV-2=severe acute respiratory syndrome-associated coronavirus 2; USA or US=United States of America; WA1=SARS-CoV-2, Isolate USA-WA1/2020.

IC_{50} values were calculated from a four-parameter dose–response curve in GraphPad Prism 8.0. The SARS-CoV-2 variants C.37 (Lambda) and B.1.621 (Mu) were evaluated at the same time while the data shown for WA1 is historical (Nonclinical Study Report PD010) [Sec. 2.6.3: 1]. The assay was performed twice. Assay 1 was performed with NHC lot [redacted]; Assay 2 was performed with lot [redacted].

Source: Nonclinical Study Report PD014 [Sec. 2.6.3: 1].

2.1.4 In Vitro Activity of NHC Against SARS-CoV-2 With Remdesivir Resistance-associated and MOV Treatment-emergent Amino Acid Substitutions in NSP12 (Polymerase) and NSP14 (Exonuclease)

A noninfectious SARS-CoV-2 reporter replicon assay was used to assess the activity of NHC against replicons encoding specific NSP12 or NSP14 substitutions (He et al, 2021) [Ref. 4.3: 06FDKT]. The SARS-CoV-2 replicon construct is replication competent and inhibited by RdRp substitutions or by known antiviral compounds in cells but lacks the structural genes to produce progeny virions,

NHC activity was evaluated against SARS-CoV-2 replicons with amino acid substitutions in NSP12 (polymerase) and NSP14 (exonuclease).

Remdesivir resistance-associated variants in the NSP12 protein (NSP12-F480L, NSP12-D484Y, NSP12-V557L, NSP12-E802A, NSP12-E802D) identified in tissue culture passaging experiments (Agostini et al, 2018; Martinot et al, 2020; Szemiel et al, 2021) [Ref. 4.3: 05K5RM], [Ref. 4.3: 06FP3F], [Ref. 4.3: 05R3M7]were tested. NHC was similarly active (EC_{50} values <1.6-fold) against replicons with remdesivir resistance-associated amino acid substitutions in NSP12 (polymerase) [Table 2.6.2: 10].

[redacted]

The treatment-emergent NSP12 and NSP14 variants NSP12-T739I, NSP14-A220S, NSP14-A220T, NSP14-A220V, NSP14-S503L, and NSP14-S503P were also evaluated. These variants were observed in NP swab samples from 3 or more participants who had received MOV in Phase 2 studies. NHC was similarly active (EC_{50} values <1.6-fold) against replicons with MOV treatment-emergent NSP12 and NSP14 (exonuclease) variants in the replicon assay [Table 2.6.2: 10].

Table 2.6.2: 10 N-Hydroxycytidine Activity Against SARS-CoV-2 With Remdesivir Resistance-associated and MOV Treatment-emergent Amino Acid Substitutions in NSP12 (Polymerase) and NSP14 (Exonuclease) in the Reporter Replicon Assay

Compound	EC_{50} (nM), Geometric Mean ± SD				
	SARS-CoV-2 Wuhan-Hu-1	NS12-F480L	NSP12-D484Y	NSP12-V557L	NSP12-T739I
NHC [a] ([redacted])	822 ± 86 (n=7)	1080 ±75 (n=8)	1290 ±121 (n=8)	369 ± 86 (n=4)	850 ± 145 (n=4)
NHC [a] ([redacted])	897 ± 201 (n=26)	1030 ± 74 (n=10)	1310 ±135 (n=10)	437 ± 58 (n=3)	825 ± 166 (n=4)
Remdesivir	15.7 ± 4.0 (n=9)	39.3 ± 3.8 (n=8)	25.6 ± 2.8 (n=8)	27.8 ± 5.7 (n=4)	19.1 ± 2.5 (n=4)
Compound	EC_{50} (nM), Geometric Mean ± SD				
	NSP12-E802A	NSP12-E802D	NSP12-F480L-V557L	NSP14-A220S	NSP14-A220T
NHC [a] ([redacted])	1050 ± 148 (n=4)	616 ± 57 (n=4)	231 ± 28 (n=3)	805 ± 67 (n=3)	1190 ± 203 (n=4)
NHC [a] ([redacted])	956 ± 146 (n=4)	648 ± 24 (n=5)	241 ± 25 (n=5)	672 ± 89 (n=4)	1190 ± 103 (n=5)
Remdesivir	17.8 ± 1.4 (n=4)	37.4 ± 2.8 (n=4)	26.1 ± 5.7 (n=4)	21.0 ± 1.8 (n=4)	21.7 ± 2.7 (n=4)
Compound	EC_{50} (nM), Geometric Mean ± SD				
	NSP14-A220V	NSP14-S503L	NSP14-S503P		
NHC [a] ([redacted])	1030 ± 164 (n=4)	1280 ± 109 (n=4)	761, 847 [b] (n=2)		
NHC [a] ([redacted])	1040 ± 95 (n=5)	1290 ± 126 (n=5)	872 ± 59 (n=4)		
Remdesivir	17.6 ± 3.3 (n=4)	18.5 ± 1.4 (n=4)	17.0 ± 0.9 (n=4)		

EC_{50} = half-maximal effective concentration; HEK = human embryonic kidney; MOV = molnupiravir or MK-4482; n = number; NHC = N-hydroxycytidine; nM = nanomolar; NSP = nonstructural protein; SARS-CoV-2 = severe acute respiratory syndrome-associated coronavirus 2; SD = standard deviation.

Amino acid single letter code: A = alanine; D = aspartic acid, E = glutamic acid; F = phenylalanine; I = isoleucine; L = leucine; P = proline; S = serine; T = threonine; V = valine; Y = tyrosine.

All assays were performed in HEK 293T cells.

[a] Two different lots of NHC were tested. The data were not aggregated.

[b] Where n<3, the individual values are listed.

Source: Nonclinical Study Report PD011 [Sec. 2.6.3: 1].

[redacted]

2.1.5 NHC Resistance Selection Studies and Antiviral Activity Against Remdesivir-resistant Mouse Hepatitis Virus Model Coronavirus and SARS-CoV

2.1.5.1 NHC Resistance Selection Against MHV and MERS-CoV

NHC was evaluated in resistance selection assays against WT MHV and WT MERS-CoV by passage in cell culture and the sensitivity of passage 30 of both MHV and MERS-CoV populations to NHC inhibition was tested (Agostini et al, 2019) [Ref. 4.3: 05JF05]. Following 30 passages, only a modest change in NHC susceptibility (approximately 2-fold increase in EC_{90}) was observed for either MHV or MERS-CoV in the presence of NHC, with replication capacities of both MHV lineages less fit than WT MHV.

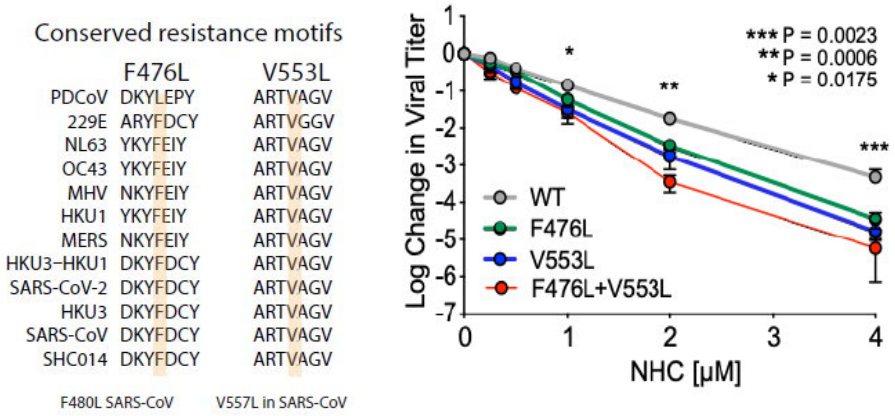
2.1.5.2 NHC Activity Against Remdesivir-resistant Viruses

CoV resistance to remdesivir was mediated by RdRp residues F476L and V553L ([Figure 2.6.2: 4], Panel A) in a model coronavirus, MHV, and in SARS-CoV, resulting in a 5-fold increase in the IC_{50} value (Agostini et al, 2018) [Ref. 4.3: 05K5RM]. RdRp sequences are highly conserved among CoV including SARS-CoV-2 (Sheahan et al, 2020) [Ref. 4.3: 05K8L0].

Two remdesivir-resistance mutations, F476L and V553L, did not confer cross resistance to NHC in an in vitro virus replication assay (Sheahan et al, 2020) [Ref. 4.3: 05K8L0]. However, the 2 mutations, alone or in combination, conferred increased sensitivity to inhibition by NHC ([Figure 2.6.2: 4], Panel B).

Figure 2.6.2: 4 Remdesivir-resistance Mutations in Coronavirus Increase Susceptibility to NHC

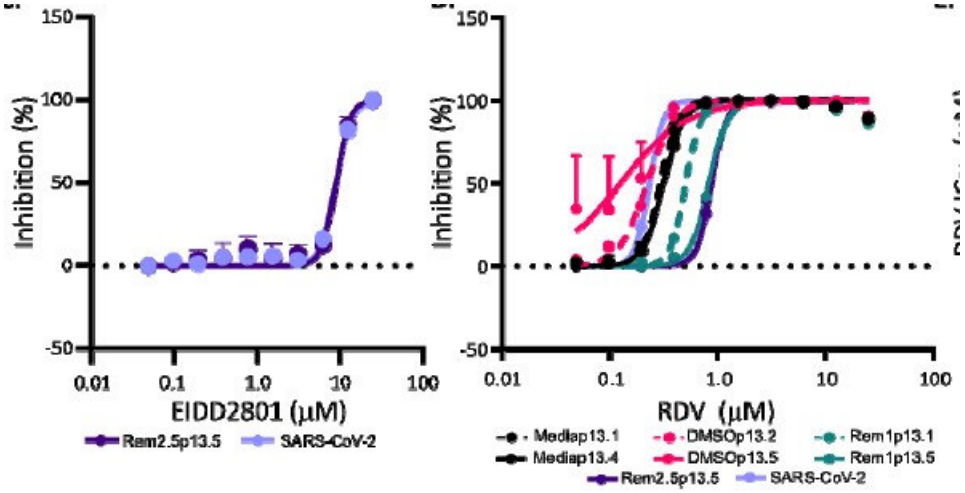
Panel A **Panel B**



DBT=murine astrocytoma delayed brain tumor; MHV=coronavirus mouse hepatitis virus; MOI=multiplicity of infection; NHC=EIDD-1931 or N-hydroxycytidine; pfu=plaque-forming unit(s); RdRp=RNA-dependent RNA polymerase; WT=wild-type.
Amino acid single letter code: F=phenylalanine; L=leucine; V=valine.
Panel A shows the amino acid sequence of coronavirus at known resistance alleles to remdesivir. In SARS-CoV these are F480L and V557L. **Panel B** shows the virus titer reduction assay results across a range of NHC concentrations with recombinant MHV bearing resistance mutations to remdesivir. Remdesivir-resistant MHVs with either 1 or both of the remdesivir-resistance mutations in the RdRp, F476L and V553L, were tested along with recombinant WT MHV strain MHV-A59 (GenBank accession number AY910861) with different concentrations of NHC in an antiviral assay. Briefly, subconfluent monolayers of DBT cells were infected with the indicated virus at MOI = 0.01 pfu/cell for 1 hour at 37°C. The inoculum was removed and replaced with medium containing the indicated concentration of NHC. Cell supernatants were harvested 24 hours post-infection. Titers were determined by plaque assay on DBT cells. Shown is the log change in viral titer by NHC concentration for each virus. Asterisks indicate statistically significant differences from WT viral titer by Mann-Whitney test.
Source: Adapted from Figure 3C and 3D in Sheahan et al, 2020 [Ref. 4.3: 05K8L0].

The activity of MOV was also evaluated in vitro against a remdesivir-resistant strain of SARS-CoV-2 in Vero E6-ACE2 cells [Ref. 4.3: 05R3M7]. SARS-CoV-2_{Engl2} was serially passaged in Vero E6 cells in media supplemented with remdesivir or normal media, resulting in resistant and partially-resistant populations of virus [Figure 2.6.2: 5]. MOV showed only a minimal change in IC_{50} against the remdesivir-resistant strain Rem2.5p13.5 (IC_{50} approximately 9.14 µM) compared with SARS-CoV-2_{Engl2} (IC_{50} approximately 8.92 µM) in contrast to remdesivir, which showed 2- to 2.5-fold increase in IC50 against the Rem2.5p13.5 strain.

Figure 2.6.2: 5 Activity of MOV Against Remdesivir-resistant SARS-CoV-2



ACE2= angiotensin-converting enzyme 2; MOV= molnupiravir, MK-4482, or EIDD-2801; pfu = plaque-forming unit; RDV = remdesivir; Rem2.5p13.5 = remdesivir-resistant strain of SARS-CoV-2; SARS-CoV-2 = severe acute respiratory syndrome-associated coronavirus 2.
Antiviral activity was assessed after infection with 8400 pfu/mL of each virus. **Lefthand panel** shows the inhibitory activity of MOV against a remdesivir-resistant strain of SARS-CoV-2 (Rem2.5p13.5) and SARS-CoV-2 in Vero E6-ACE2 cells. **Righthand panel** shows the inhibitory activity of remdesivir against a remdesivir-resistant strain of SARS-CoV-2 (Rem2.5p13.5) and SARS-CoV-2 in A549NPro-ACE2 cells. Also shown are activity against control viruses Mediap13.1, Mediap13.4, DMSOp13.2, and DMSOp13.5, and viruses with reduced sensitivity to remdesivir, Rem1p13.1 and Rem1p13.5.
Source: Adapted from Panels C and D from Figure 1 in Szemiel et al, 2021 [Ref. 4.3: 05R3M7].

2.1.6 In Vitro Evaluation of NHC Uptake by Cell Lines, by Human, Dog, and Rat PBMCs and in HBEC Air-liquid Interface Cultures

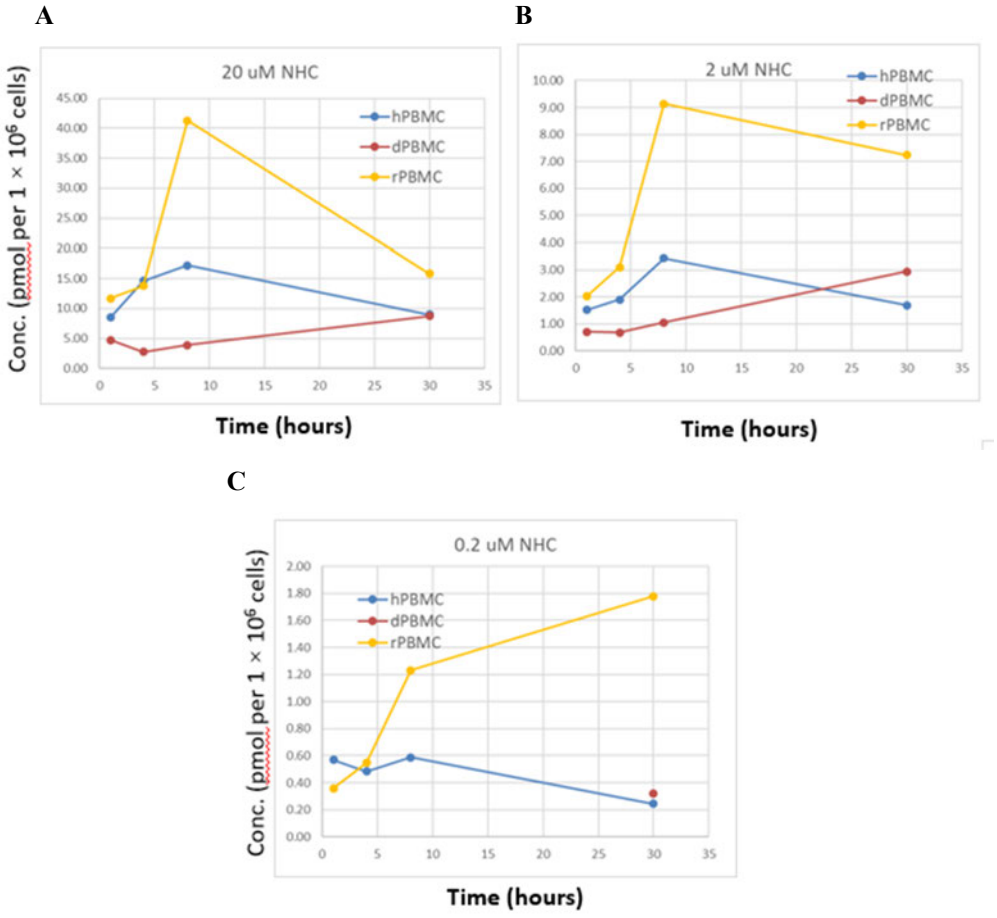
The uptake and phosphorylation of NHC were investigated to determine the intracellular concentrations of phosphorylated forms in cell lines, in human, dog, and rat PBMCs, and in HBEC ALI cultures and described in Nonclinical Study Report PD012 [Sec. 2.6.3: 1]. The cell lines included 293T, Vero, A549, Calu-1, and Huh-7.5. Determination of the intracellular concentrations and persistence of NHC-MP, NHC-DP, and NHC-TP following incubation with NHC for 24 hours were also studied.

NHC was efficiently taken up by cell lines, PBMCs, and HBEC ALI cultures, and phosphorylated to mono-, di-, and tri-phosphate forms. The phosphorylated forms of NHC are catabolized in a few hours in cell lines and PMBCs after 24 hours of treatment with NHC.

NHC-TP was rapidly metabolized in HBEC ALI cultures by 24 hours after removal of NHC, with NHC-TP concentrations higher than for NHC-DP or NHC-MP. NHC-TP was detectable at least 24 hours after treatment with 10 µM NHC in HBEC ALI cultures.

NHC was efficiently phosphorylated to NHC-TP in a dose-dependent manner in human, dog, and rat PBMCs as shown in [Figure 2.6.2: 6].

Figure 2.6.2: 6 Time Course Profile of Intracellular NHC-TP Concentrations After Treatment of Human, Dog, or Rat PBMCs With 0.2, 2, or 20 µM NHC



Conc.= concentration; dPBMC=dog PBMCs; hPBMC=human PBMCs; NHC=N-hydroxycytidine; NHC-TP=triphosphate form of NHC; PBMC=peripheral blood mononuclear cell; pmol=picomole(s); rPBMC=rat PBMCs.

Shown are graphical representations of the intracellular NHC-TP concentration data for treatment with 20 µM NHC (**Panel A**), 2 µM NHC (**Panel B**), or 0.2 µM NHC (**Panel C**). Data for human PBMCs are shown in blue, data for dog PBMCs are shown in red, and data for rat PBMCs are shown in yellow. The dog PBMCs tended to clump during the experiment. The dog PBMC results may be impacted.

Source: Figure 3 in Nonclinical Study Report PD012 [Sec. 2.6.3: 1].

2.1.7 Cytotoxicity of NHC in Tissue Culture Utilizing Cells From Different Organs and Species

NHC was tested for cytotoxicity in human hepatic origin Huh7 and HepG2 cells, in human lymphoid CEM, human pancreatic BxPC-3, human prostate cancer PC-3, human muscle A204, human lung A549, human epithelial HEp-2, rat heart muscle H9c-2, monkey kidney Vero, and MDCK cell lines [Table 2.6.2: 11]. NHC exhibits low cytotoxicity in the tested cells [CC_{50} values of 7.5 to >100 µM, (Sticher et al, 2020; Yoon et al, 2018) [Ref. 4.3: 05JF0B], [Ref. 4.3: 05JF0G] well above the NHC EC_{50} for antiviral activity against SARS-CoV-2 in various cell lines in vitro (EC_{50} = 0.32 to 2.66 µM; [Table 2.6.2: 3]).

Table 2.6.2: 11 Cytotoxicity (CC_{50}) of NHC in Mammalian Cell Lines

Cell Line	CEM	HepG2	PC-3	A204	A549	BxPC-3	Huh-7	H9c-2	Vero	HEp-2	MDCK
CC_{50} (µM)	7.5	42.3	267.1	84	46	48	165.5	81	53	272.4	299.8

CC_{50}=half-maximal cytotoxicity concentration; MDCK=Madin-Darby Canine Kidney; µM=micromolar; NHC=EIDD-1931 or N-hydroxycytidine.
Source: Sticher et al, 2020; Yoon et al, 2018 [Ref. 4.3: 05JF0B], [Ref. 4.3: 05JF0G].

MOV and NHC were also evaluated for potential in vitro cytotoxicity against 10 cell lines, including EKVX (human lung adenocarcinoma), SF268 (human glioblastoma), CCD1072SK (normal human foreskin fibroblasts), HeLa (human cervical adenocarcinoma), CEM-SS (human T lymphoblastoid), U87MG (human glioblastoma), MRC5 (human male diploid embryonal lung fibroblast), A549 (human lung carcinoma), SKNAS (human neuroblastoma) and Huh7 (human liver carcinoma) (Nonclinical Study Report PD009) [Sec. 2.6.3: 1]. MOV showed no cytotoxicity at concentrations up to 100 µM with any of the cell lines (CC_{50} >100 µM). NHC yielded CC_{50} values of 88.5 µM, 96.5 µM, and 95.3 µM for CCD1072SK, HeLa, and U87MG cells, respectively. NHC did not reduce cell viability by ≥50% for any of the remaining 7 cell lines, with CC_{50} >100 µM.

2.1.8 Assessment of Mitochondrial Toxicity

The potential of NHC-TP to be incorporated into mitochondrial RNA by mitochondrial RNA polymerase has been investigated and reported by Sticher et al., 2020 [Ref. 4.3: 05JF0B]. Overall, the authors show that NHC-TP incorporation into mitochondrial RNA by the mitochondrial DNA-dependent RNA polymerase (POLRMT) is 740-times less efficient than that of the natural CTP, and does not result in toxicity or dysfunction of mitochondria in vitro.

2.1.9 In Vitro Evaluation of MOV on Human Myeloid and Erythroid Colony Forming Cell Assays (PD006)

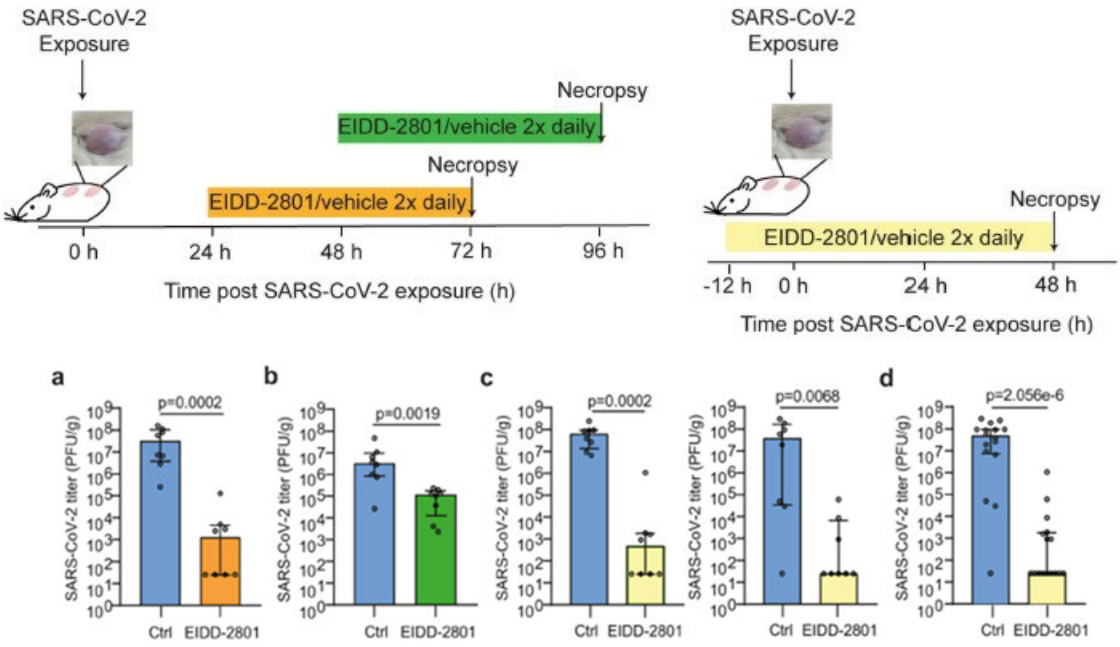
The potential effects of MOV on erythroid and myeloid progenitor proliferation were evaluated in a semi-solid methylcellulose-based culture system supporting the proliferation of human erythroid and myeloid progenitors (Nonclinical Study Report PD006) [Sec. 2.6.3: 1]. MOV inhibited erythroid progenitor proliferation at 50 and 20 µM and myeloid progenitor proliferation at 50, 20, 10, and 5 µM. This resulted in IC_{50} values of 24.9 and 7.7 µM for erythroid and myeloid progenitor proliferation, respectively. Based on the IC_{50} data, MOV had a greater inhibitory effect on the myeloid as compared to the erythroid progenitors. The internal control (5′-fluorouracil) behaved as expected. This assay is designed to detect acute hematopoietic effects following exposure to MOV. No hematologic effects indicative of bone marrow toxicity were noted in clinical trials, and this in vitro erythroid and myeloid progenitor proliferation data are not considered relevant in clinical use.

2.2 In Vivo Pharmacology

2.2.1 MOV Activity Against SARS-CoV-2 in a Pre-exposure Prophylaxis and Post-exposure Therapeutics Lung Only Mouse Model

MOV significantly reduced infectious SARS-CoV-2 levels in lung tissue from infected mice harboring human lung implants (Lung only Mice, LoM) (Wahl et al, 2021) [Ref. 4.3: 05R3M8]. LoM mice were orally administered MOV (500 mg/kg) or vehicle control, 12 hours prior, 24 hours post, or 48 hours post direct infection of human lung tissue with SARS-CoV-2, followed by twice daily dosing for up to 48 hours. Lung tissue was harvested 48 hours following infection or initiation of treatment and SARS-CoV-2 titers were determined. Both pre-exposure prophylaxis ([Figure 2.6.2: 7], lower Panels c and d) and post exposure treatment ([Figure 2.6.2: 7], lower Panels a and b) with MOV significantly reduced infectious SARS-CoV-2 levels in lung tissue recovered from mice in separate experiments. These results provide further evidence of the direct effect of MOV on SARS-CoV-2 replication.

Figure 2.6.2: 7 Pre-exposure Prophylaxis and Post-exposure Treatment With MOV (EIDD-2801) Potently Prevents SARS-CoV-2 Infection In Vivo



Abbreviations: Ctrl=control; EIDD-2801 = MK-4482, MOV, or molnupiravir; h = hour(s); LoM=lung only mice; SARS-CoV-2=Severe acute respiratory syndrome-associated coronavirus 2.

Upper panels: Experimental design. Lung only Mice (LoM) were administered MOV or vehicle control 24 or 48 hours post-infection and every 12 hours thereafter (left panel) or 12 hours prior to SARS-CoV-2 exposure and every 12 hours thereafter (right panel). Virus titers in human lung tissues were measured 2 days after the initiation of treatment (left panel) or 2 days post-exposure (right panel).

Lower panels: Shown are the SARS-CoV-2 titers in the human lung tissue of LoM administered MOV or vehicle (control) at 24 hours (panel a) or 48 hours (panel b) post-virus exposure (n = 8 per group). Panels c and d show SARS-CoV-2 titers in human lung tissue of LoM administered MOV or control vehicle at 2 days post-exposure in 2 independent experiments (panel c, separate; panel d, combined). Titers were compared with a two-tailed Mann-Whitney U test. Horizontal and vertical lines represent the median and interquartile range respectively.

Source: Top panel adapted from Extended Data Figure 4; bottom panel adapted from Figure 4, Wahl et al, 2021 [Ref. 4.3: 05R3M8].

2.2.2 Activity Against SARS-CoV-2 in a Ferret Model of Coronavirus Infection

The efficacy of MOV to mitigate SARS-CoV-2 infection and block transmission was examined in a ferret model of coronavirus infection (Cox et al, 2020) [Ref. 4.3: 05NRF7]. High levels of SARS-CoV-2 virus can be detected in nasal tissues and secretions from ferrets after intranasal infection with 1×10^5 pfu of SARS-CoV-2 (2019-nCoV-USA-WA1-2020); these high virus levels coincide with viral transmission through direct contact in this model. Treatment of infected ferrets with MOV twice daily significantly reduced the SARS-CoV-2 viral load in the upper respiratory tract and completely suppressed viral spread to untreated contact animals. MOV significantly reduced virus titers in nasal lavages of infected ferrets within 12 hours of treatment in all treatment groups (either 5 or 15 mg/kg twice daily starting 12 hours post-infection, or 15 mg/kg twice daily starting 36 hours post-infection;

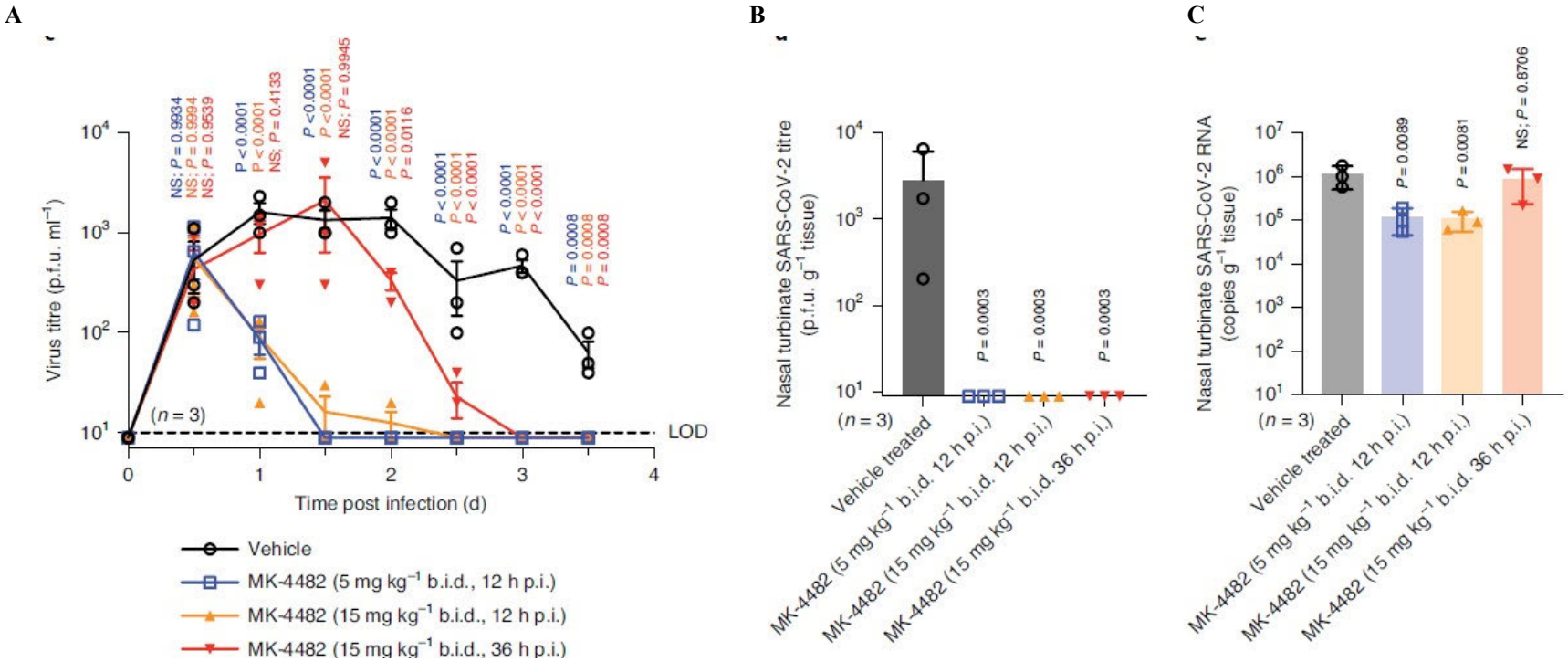
[Figure 2.6.2: 8], Panel A). Evaluation of nasal turbinates for infectious particles 4 days post-infection confirmed the antiviral impact of MOV treatment ([Figure 2.6.2: 8], Panel B), although viral RNA was still detectable ([Figure 2.6.2: 8], Panel C).

In a second study to examine the impact of MOV treatment on viral transmission, ferrets were infected as before and treated with MOV at 5 mg/kg twice daily or vehicle starting 12 hours post-infection. After 30 hours, each ferret was co-housed with 2 un-infected untreated contact ferrets. After 3 days the originally infected/treated animals were euthanized, and contact ferrets isolated and monitored for an additional 4 days. The contact ferrets of vehicle-treated infected animals began to shed SARS-CoV-2 within 20 hours of co-housing [Figure 2.6.2: 9]. No virus (infectious particles or RNA) was detected in the untreated contacts of source ferrets that had been treated with MOV [Figure 2.6.2: 9].

In summary, treatment with MOV reduced SARS-CoV-2 infectious viral titers in nasal secretions from infected ferrets and suppressed all viral transmission to the untreated direct contacts, despite prolonged direct proximity between source and contact animals.

[redacted]

Figure 2.6.2: 8 Therapeutic Oral Administration of MOV is Efficacious Against SARS-CoV-2 in a Ferret Infection Model



ANOVA=analysis of variance; d=day(s); g=gram(s); h=hours; mg kg^{-1} or mg/kg=milligram per kilogram; mL=milliliter(s); MOV=molnupiravir or MK-4482; n=number; pfu=plaque-forming unit(s); p.i.=post-infection; RNA=ribonucleic acid; SARS-CoV-2=severe acute respiratory syndrome-associated coronavirus 2.

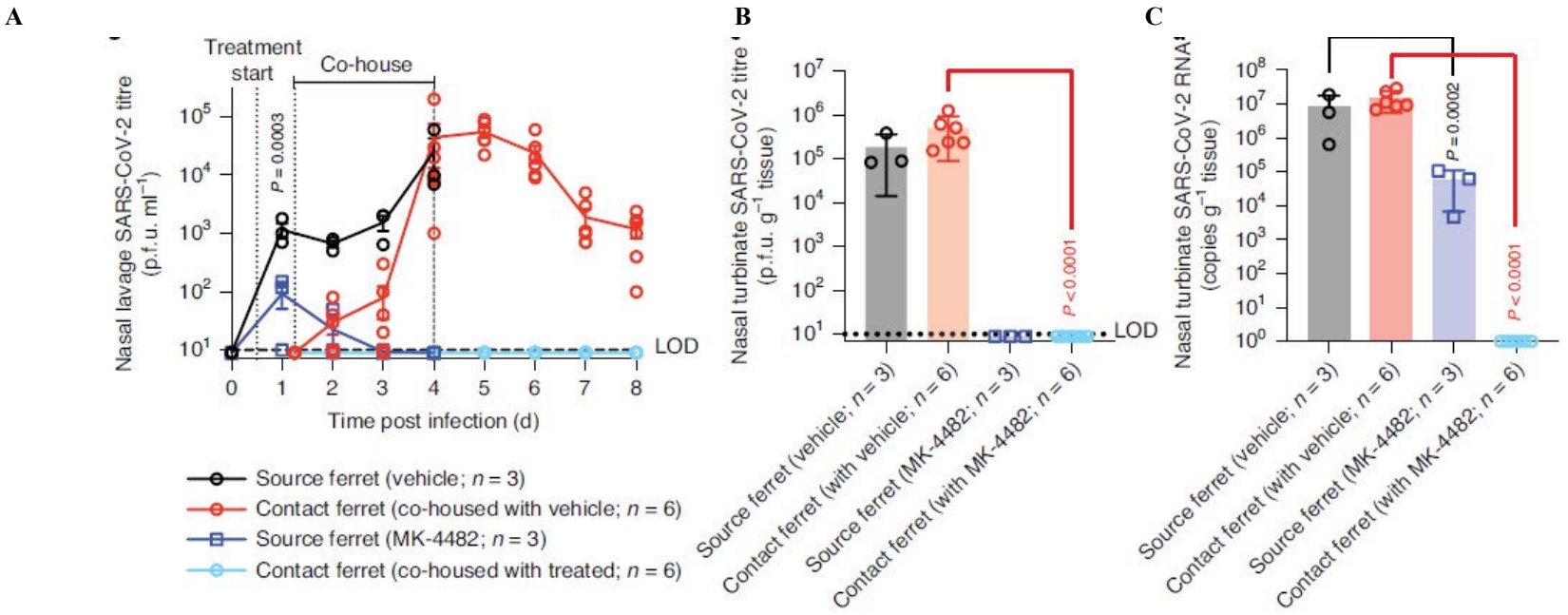
Ferrets were infected intranasally with 1×10^5 pfu 2019-nCoV/USA-WA1/2020 SARS-CoV-2 and orally gavaged with either vehicle or MOV twice daily beginning 12 hours post-infection (5 mg/kg or 15 mg/kg MOV) or at 36 hours post-infection (15 mg/kg MOV). Nasal lavages were collected twice a day. **Panel A** shows the viral titers of nasal lavages of infected ferrets. MOV treatment significantly reduced virus titers within 12 hours of dosing onset in all treatment groups. Statistical analysis was performed using 2-way ANOVA with Dunnett's multiple comparison post-hoc test. **Panel B** shows the infectious particle numbers and **Panel C** shows the viral RNA copy numbers in the nasal turbinates of infected ferrets 4 days post-infection. Statistical analysis was performed using a one-way ANOVA with Dunnett's multiple comparison post-hoc test. *P*-values are shown; symbols represent individual animals and lines connect the group mean ± standard deviation (Panel A). Bar graphs show the mean ± standard deviation (Panels B and C).

Source: Adapted from Panels C, D, and E of Figure 2 in Cox et al, 2020 [Ref. 4.3: 05NRF7].

[redacted]

C Confidential

Figure 2.6.2: 9 Therapeutic Oral Administration of MOV Prevents Contact Transmission of SARS-CoV-2 in a Ferret Infection Model



ANOVA=analysis of variance; d=day(s); g=gram(s); mg/kg=milligram per kilogram; mL=milliliter(s); MOV=molnupiravir or MK-4482; n=number; pfu=plaque-forming unit(s); RNA=ribonucleic acid; SARS-CoV-2=severe acute respiratory syndrome-associated coronavirus 2.

Ferrets were infected intranasally with 1×10^5 pfu 2019-nCoV/USA-WA1/2020 SARS-CoV-2 and orally gavaged with either vehicle or 5 mg/kg MOV twice daily beginning 12 hours post-infection. After 30 hours post-infection, each source ferret was co-housed with 2 uninfected untreated contact ferrets. Nasal lavages were collected once a day. The source animals were euthanized after 3 days of co-housing, and the contact ferrets were isolated and monitored for an additional 4 days. **Panel A:** Source ferrets treated with MOV had significantly lower virus titers than vehicle-treated animals within 12 hours after treatment (p=0.0003). Contacts of vehicle-treated source ferrets began to shed SARS-CoV-2 within 20 hours of co-housing. Statistical analysis was performed using 2-way ANOVA with Sidak's multiple comparison post-hoc test. **Panel B** shows the infectious particle numbers and **Panel C** shows the viral RNA copy numbers in the nasal turbinates of the source and contact ferrets extracted 4 and 8 days after the study start, respectively. Statistical analysis was performed using a one-way ANOVA with Sidak's multiple comparison post-hoc test. *P*-values are shown. For Panel B, $p<0.0001$ for intergroup comparison of contact animals; for Panel C, p=0.0002 and $p<0.0001$ for intergroup comparisons of the source and contact animals, respectively.

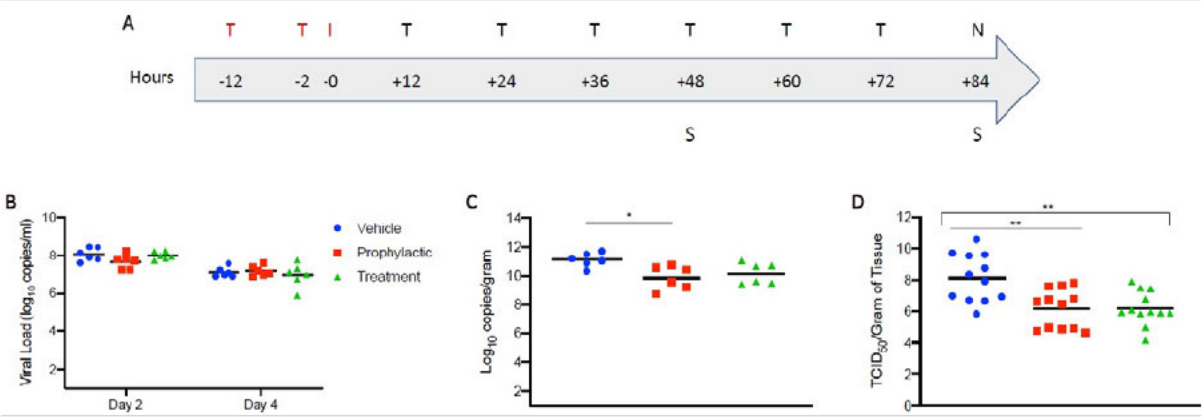
Source: Adapted from Panels B, C, and D of Figure 3 in Cox et al, 2020 [Ref. 4.3: 05NRF7].

[redacted]

2.2.3 MOV Reduces SARS-CoV-2 Viral RNA and Infectious Virus Titers in Lung Tissues in a Syrian Hamster Model of Infection

In a Syrian hamster model of SARS-CoV-2 infection and disease, MOV prophylactic or therapeutic treatment of hamsters infected with SARS-CoV-2 showed decreased viral RNA titers and infectious virus from lungs several days post infection [Figure 2.6.2: 10] (Rosenke et al, 2021) [Ref. 4.3: 05R3LW]. In addition, histopathological analysis of lung tissue harvested after infection showed significantly reduced SARS-CoV-2 nucleocapsid antigen levels and a lower abundance of pulmonary lesions in MOV-treated animals compared with vehicle controls (data not shown).

Figure 2.6.2: 10 Syrian Hamster Model Study Design, Viral Shedding, Viral Load, Infectious Titers, and Viral Antigen



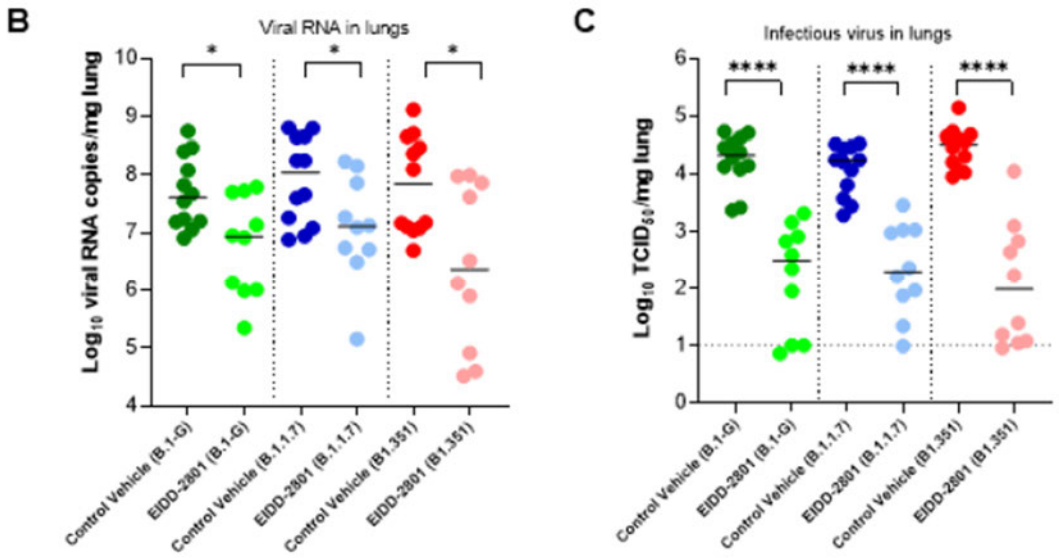
Abbreviations: ANOVA = analysis of variance; I = infection; MOV=molnupiravir or MK-4482; N = necropsy; RT-PCR = reverse transcriptase polymerase chain reaction; S = swab samples; SARS-CoV-2 = severe acute respiratory syndrome-associated coronavirus 2; T = treatment; $TCID_{50}$ = 50% tissue culture infectious dose.
Panel A: Study design. Hamsters were infected with SARS-CoV-2 by the intranasal route. MOV was administered either pre-infection at 12 and 2 hours prior to infection, or post-infection with treatment started 12 hours post-infection. Treatment was continued in both treatment groups every 12 hours for 3 consecutive days until the end of the experiment. Animals were euthanized on Day 4 and lungs harvested for pathology and virology. Red indicates pre-infection; black indicates post-infection treatments. **Panel B: Viral shedding**. Oral swabs were collected on Days 2 and 4 post-infection to measure viral shedding, determined by RT-PCR (N gene: genomic and subgenomic). **Panel C: Viral load in lung tissue**. Lung viral loads based on RT-PCR (N gene: genomic and subgenomic) were determined as a correlate for lower respiratory tract infection. **Panel D: Infectious titer in lung tissue**. Lung samples were homogenized and titered on Vero E6 cells. Infectious titers were determined as $TCID_{50}$ equivalents using the Reed-Muench method. Two independent lung samples were measure from each animal (n=12). **Panels B through D**: Blue circle, vehicle control; red square, pre-infection treatment; green triangle, post-infection treatment. Geometric means are shown. ANOVA followed by Kruskal-Wallis analysis and a pairwise Wilcox test was used to analyzed differences among groups. * = $p<0.05$; ** = $p<0.008$.
Source: Adapted from Figure 2 in Rosenke et al, 2021 [Ref. 4.3: 05R3LW].

2.2.4 MOV Inhibits Replication of SARS-CoV-2 Variants of Concern in a Syrian Hamster Model of Infection

In Syrian hamsters infected with 1×10^5 $TCID_{50}$ units of either the B.1-G (Wuhan strain), B.1.1.7 (Alpha), or B.1.351 (Beta) variants of SARS-CoV-2, treatment with 200 mg/kg BID

MOV resulted in statistically significant reductions in viral RNA copies per mg of lung tissue ([Figure 2.6.2: 11], panel B). Treatment also significantly reduced infectious virus lung titers regardless of variant ([Figure 2.6.2: 11], panel C). There was a significant improvement of cumulative histopathological lung scores in all MOV-treated groups with a reduction of median disease scores from 9.5 to 5.3 (p=0.0004), 7.8 to 5.2 (p=0.001), 8.0 to 4.3 (p=0.013) for the Wuhan, B.1.1.7 (Alpha), and B.1.351 (Beta) strains, respectively. Lungs of MOV-treated animals showed no or very focal bronchopneumonia, no or focal perivascular inflammation, and no perivascular edema (Abdelnabi et al, 2021) [Ref. 4.3: 06FGX5].

Figure 2.6.2: 11 MOV Reduces Viral Loads in Syrian Hamsters Infected With Different SARS-CoV-2 Variants



BID = twice daily; MOV=molnupiravir or MK-4482 or EIDD-2801; RNA = ribonucleic acid; SARS-CoV-2 = severe acute respiratory syndrome-associated coronavirus 2; $TCID_{50}$ = 50% tissue culture infectious dose.

In this figure MOV is labeled as EIDD-2801. **Panel B:** Viral RNA levels in the lungs of vehicle-treated (BID) animals and MOV-treated (200 mg/kg, BID) hamsters infected with 1×10^5 $TCID_{50}$ units of Wuhan (B.1-G), B.1.1.7 (Alpha), or B.1.351 (Beta) SARS-CoV-2 strains at Day 4 post-infection are expressed as log10 SARS-CoV-2 RNA genome copies per mg lung tissue. Individual data and median values are shown. **Panel C:** Infectious viral loads in the lungs of vehicle-treated) and MOV-treated hamsters infected with different SARS-CoV-2 variants at Day 4 post-infection are expressed as log10 $TCID_{50}$ per mg lung tissue. Individual data and median values are shown. All data were analyzed with the Mann-Whitney U test where * = p<0.05, ** = p<0.01, *** = p<0.001, and **** = p<0.0001. Data are from 2 independent experiments. The number of animals were 12 and 10 per vehicle and MOV-treated groups, respectively. Only panels B and C are shown.

Source: Adapted from Figure 1 in Abdelnabi et al, 2021 [Ref. 4.3: 06FGX5].

2.2.5 SARS-CoV-1 and MERS-CoV

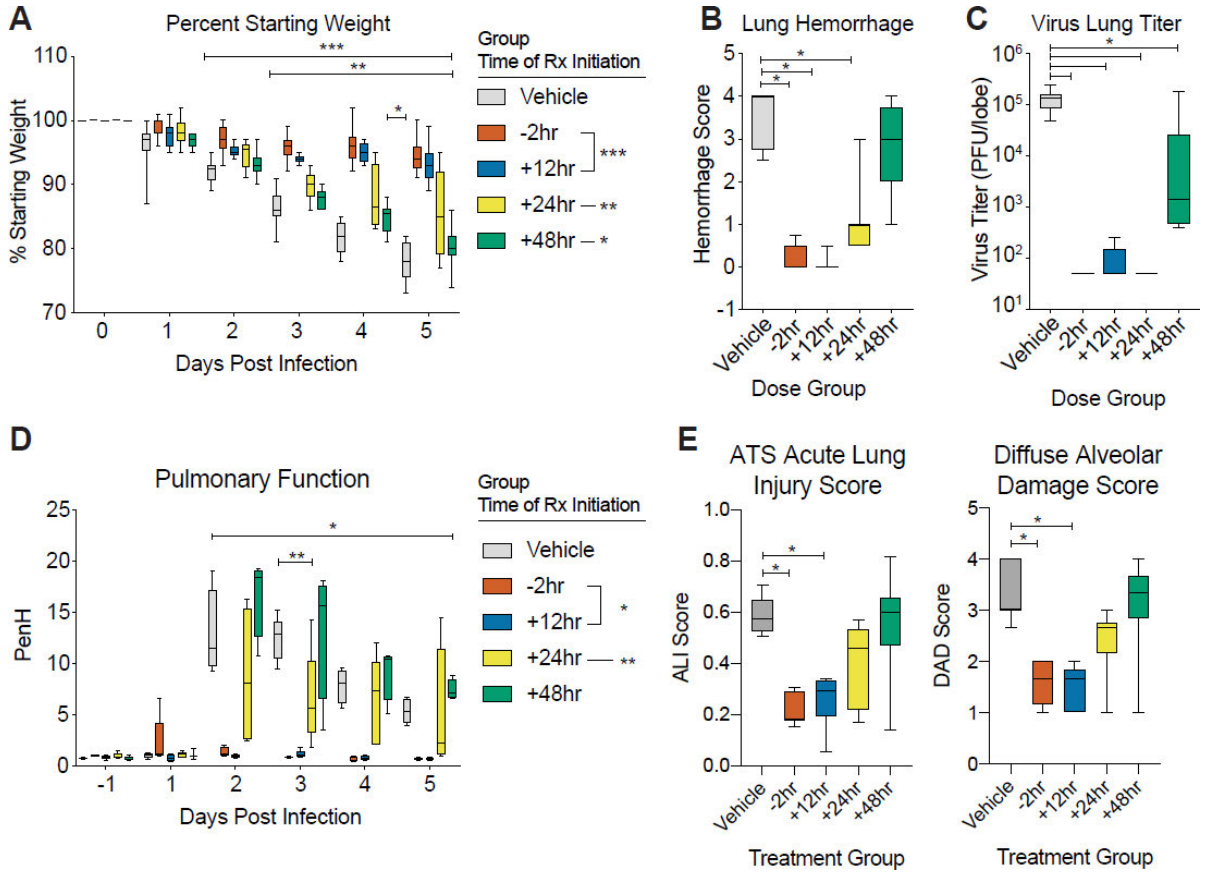
In mice infected with either SARS-CoV-1 or MERS-CoV, prophylactic or therapeutic treatment with MOV reduced body weight loss and virus replication and improved pulmonary function (Sheahan et al, 2020) [Ref. 4.3: 05K8L0].

In a prophylactic dose-escalation study in C57BL/6 mice, MOV (50, 150, or 500 mg/kg) or vehicle was administered 2 hours prior to intranasal infection with SARS-CoV (SARS-MA15) and then every 12 hours thereafter for 5 days post-infection. A dose-dependent reduction in SARS-CoV lung titer was observed with significant differences between the vehicle (6.5×10^4 pfu/mL), 150 mg/kg MOV (2.5×10^3 pfu/mL), and 500 mg/kg MOV (50 pfu/mL) groups. MOV significantly diminished (50 mg/kg) or prevented (150, 500 mg/kg) body weight loss and reduced lung hemorrhage (500 mg/kg) compared to vehicle-treated animals.

In a follow-up study in C57BL/6 mice, a 500 mg/kg dose of MOV was given 2 hours prior to infection, or at 12, 24, or 48 hours after infection with 1×10^4 pfu SARS-MA15 and then every 12 hours for 5 days post-infection [Figure 2.6.2: 12]. Significantly reduced lung viral loads were observed for each of the MOV groups compared with vehicle-treated animals. Treatment at -2 hours pre-infection or at 12 hours post-infection significantly reduced body weight loss, reduced lung hemorrhage, and improved pulmonary function compared to vehicle-treated animals. Later initiation of dosing (24 or 48 hours) showed less benefit for preventing body weight loss and lung hemorrhage in infected animals.

In hDPP4 288/330 mice, administration of MOV (50, 150, and 500 mg/kg) from 2 hours before infection with MERS-CoV (mouse-adapted virus) prevented body weight loss, lung hemorrhage, and viral replication ($p<0.0001$ by 5 days post-infection) compared with vehicle-treated animals. With therapeutic dosing, viral lung titer measured 6 days after infection was significantly reduced to limit of detection for all treatment initiation times. Administration of MOV ≤12 hours, though not at later times after MERS-CoV infection, prevented body weight loss and lung hemorrhage.

Figure 2.6.2: 12 Prophylactic and Therapeutic Treatment With MOV Reduces SARS-CoV Replication and Pathogenesis in Mice



ALI=acute lung injury; ANOVA=analysis of variance; ATS=American Thoracic Society; DAD=diffuse alveolar damage; hr=hour(s); MOV=molnupiravir or MK-4482; pfu=plaque-forming unit(s); PenH=enhanced pause; Rx=treatment; SARS-CoV=severe acute respiratory syndrome-associated coronavirus.

Mice were intranasally infected with mouse-adapted SARS-CoV MA15 strain. **Panel A**, Percent starting weight (n=10). **Panel B**, Lung hemorrhage in mice from panel A scored on a scale of 0 to 4 where 0 is a normal pink healthy lung and 4 is a diffusely discolored dark red lung. **Panel C**, Virus lung titer in mice from Panel A as determined by plaque assay. **Panel D**, Pulmonary function by whole body plethysmography was performed daily on five animals per group. **Panel E**, Therapeutic administration of MOV reduces acute lung injury. Asterisks in panels A through D indicate differences by ANOVA with Tukey's (A) Dunnett's (B-D) multiple comparison test. Asterisks indicate statistical significance compared to vehicle by Kruskal-Wallis with a Dunn's multiple comparison test (E).

Source: Adapted from Figure 6 in Sheahan et al, 2020 [Ref. 4.3: 05K8L0].

2.2.6 Influenza Virus

Studies in a ferret model of influenza virus infection demonstrated that administration of MOV provided therapeutic benefit against IAV (H1N1). MOV in doses of 0.8, 2.3, or 7 mg/kg (3.5-mL) by oral gavage BID was tested in a ferret model of influenza virus infection and disease (Toots et al, 2020) [Ref. 4.3: 05JF09]. Animals were infected intranasally with 1×10^5 pfu (200 µL) of IAV H1N1 virus and MOV dosing was initiated 12 hours later. Treatment with 7 mg/kg BID led to a reduction in shed virus load by multiple orders of magnitude, and alleviated fever and inflammation while improving airway

epithelium histopathology. Treatment with 2.3 mg/kg BID resulted in moderate reduction of virus titer but no significant reduction of fever. The 0.8 mg/kg dose BID had no significant therapeutic effect. By 48 hours post-infection, the disease in ferrets begins to self-resolve; therefore, initiating treatment up to 36 hours post-infection allows for detection of antiviral activity before self-resolution of disease. Administered in 12-hours intervals, three 7 mg/kg doses of MOV were sufficient for maximal therapeutic benefit against a pandemic IAV (H1N1) and significantly shortened the time to resolution of clinical signs. Ferrets infected with pandemic IAV and treated with MOV at a dose of 7 mg/kg demonstrated significantly less viral shedding and inflammatory cellular infiltrates in nasal lavages but mounted a normal humoral antiviral response (Toots et al, 2020) [Ref. 4.3: 05JF09]. A similar study using ferrets infected intranasally with 1×10^6 pfu (200 µL) of IAV H3N2 virus demonstrated the same results for MOV (0.8, 2.3, or 7 mg/kg by oral gavage BID) in the seasonal IAV model.

When examining the effect of delayed dosing in a different study in the same pandemic IAV ferret model (H1N1), Toots et. al., 2019 [Ref. 4.3: 05JF0D] demonstrated that treatment with 20 mg/kg of MOV initiated 24 hours after challenge with IAV (H1N1) resulted in a rapid decrease in both shed virus and fever relative to control, with fever returning to baseline at 24 hours [Figure 2.6.2: 13]. When oseltamivir (20 mg/kg) was dosed prophylactically as a positive control, a modest suppression of fever was observed; however, there was no reduction in shed virus titer (as measured by both infectious units and by reverse transcriptase polymerase chain reaction).

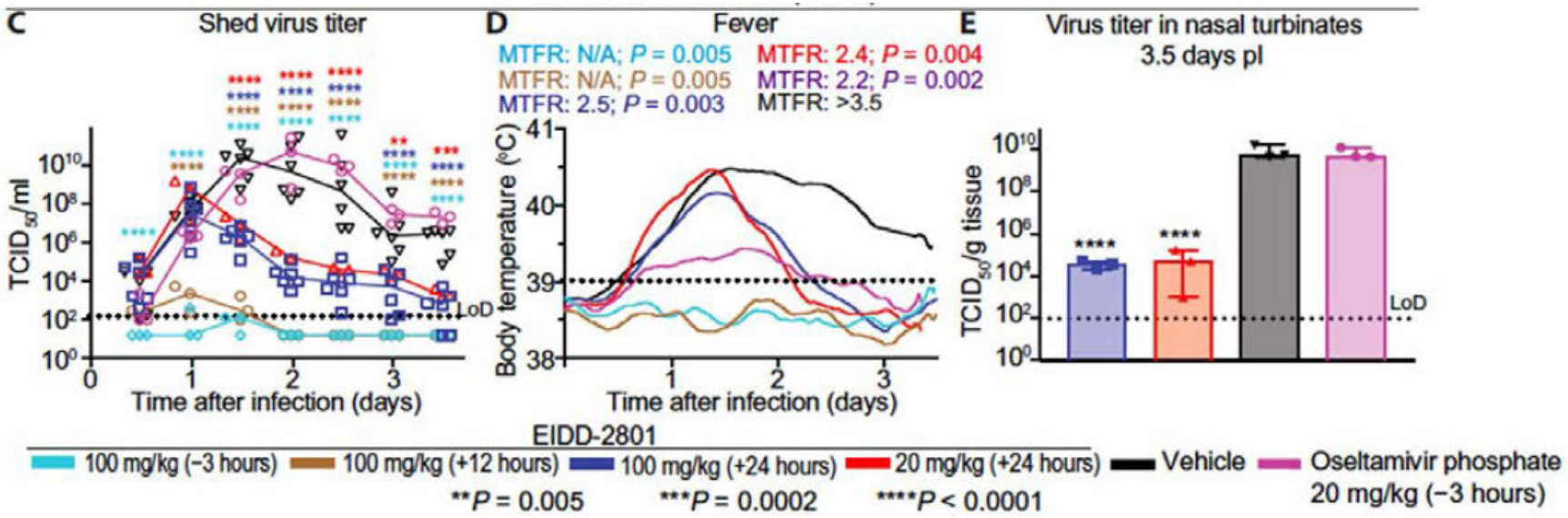
2.2.7 Venezuelan Equine Encephalitis Virus

Treatment with NHC was evaluated in a mouse model of lethal VEEV infections. High plasma levels of NHC are rapidly achieved in mice after oral dosing and distributes into organs important in the pathology of VEEV infection, including the brain. In mouse model studies of VEEV infection, NHC was 90% to 100% effective in protecting mice against lethal intranasal infection when therapeutic treatment was started as late as 24 hours post-infection, and partial protection was achieved when treatment was delayed for 48 hours post-infection (Painter et al, 2019) [Ref. 4.3: 05JM4T].

2.2.8 Ebola Virus

NHC showed specific antiviral activity against EBOV in tissue culture (EC_{50} = 3.8 to 4.7 µM) (Reynard et al, 2015; erratum, 2016; Nonclinical Study Report PD002 ([redacted] STDY-16-0019-JC)) [Ref. 4.3: 06CK43] [Sec. 2.6.3: 1]. In a mouse model testing a lethal EBOV challenge, NHC dosed BID at 200 mg/kg for 7 days resulted in 100% survival, when the treatment was initiated therapeutically starting at 6 hours post-infection. Treated animals demonstrated recovery of body weight loss and reduced clinical signs of Ebola virus disease. The study is summarized in Nonclinical Study Report PD002 ([redacted] STDY-16-0019-JC) [Sec. 2.6.3: 1].

Figure 2.6.2: 13 Antiviral Activity of MOV in the Ferret Model of Influenza (A/California/07/2009[H1N1])



EIDD-2801 = MK-4482, MOV, or molnupiravir; LoD=limit of detection; MTFR=median time to resolve fever; N/A=not applicable; pI=post-infection; $TCID_{50}$=50% tissue culture infectious dose.

In this figure MOV is labeled as EIDD-2801.

Source: Adapted from Toots et al, 2019, Figure 1, panels C, D, and E with underlying table only. [Ref. 4.3: 05JF0D].

[redacted]

3 SECONDARY PHARMACODYNAMICS

NHC was tested in an assay at [redacted] ([redacted], USA) for inhibition potential against a panel of ion channels, including Cav1.2 (CYL5051QU), HCN4 (CYL5012HT), hERG (CYL5038), KCNQ1/minK (CYL5007QU), Kir2.1 (CYL5032QU), Kv1.5 (CYL5018QU), Kv4.3/KChlP2 (CYL5069QU), and Nav1.5 (Cardiac Protocol) (CYL5004QU) (Nonclinical Study Report PD003 [[redacted] Report No. EMO022216-1]) [Sec. 2.6.3: 1]. There was no observed inhibition of function of any ion channel tested with NHC at 10 µM in this study. A number of positive and negative controls were run in tandem and all behaved as expected, indicating that the assay results are reliable.

In a second larger study (Nonclinical Study Report PD004) [Sec. 2.6.3: 1], neither MOV nor NHC exhibited ≥50% inhibition at 10 µM against 107 of the 108 enzymes, receptors, or ion channels tested. MOV and NHC inhibited COX-2 by 62% and 52%, respectively, at 10 µM, with estimated IC_{50} values of 6.33 µM and 15.1 µM, respectively. MOV IC_{50} is 243-fold above the MOV clinical C_{max} (0.026 µM) at the 800 mg Q12H dose. NHC IC_{50} is 5.7- to 47-fold above the NHC EC_{50} for antiviral activity against SARS-CoV-2 in various cell lines in vitro (EC_{50} = 0.32 to 2.66µM; [Table 2.6.2: 3]) and also above the clinical C_{max} (10.8 µM) at the human dose of 800 mg Q12H.

The effect of NHC-TP on the enzymatic activity of human DNA polymerases α, β, and γ was assessed in biochemical assays using concentrations of dNTPs significantly lower than physiological, intracellular dNTP concentrations (Nonclinical Study Report PD013) [Sec. 2.6.3: 1]. NHC-TP had IC_{50} values of 20.7 µM, 7.48 µM, and 56.4 µM, respectively, for human DNA polymerases α, β, and γ, under low dNTP concentrations. Given the dNTP concentrations used in the optimized assay are lower than would be expected intracellularly, the Cheng-Prusoff equation was used to determine the IC_{50} value that would be expected under physiological concentrations of dNTPs. The IC_{50} values calculated to be obtained under physiological concentrations of dNTPs were >1000 µM for the three DNA polymerases.

4 SAFETY PHARMACOLOGY

Safety pharmacology studies consistent with recommendations from the ICH S7A and S7B guidelines were performed in both in vitro and in vivo test systems to assess the potential cardiovascular, respiratory, and neurobehavioral effects of MOV [Table 2.6.2: 12]. All pivotal safety pharmacology studies were conducted in accordance with the principles of GLP. All studies were conducted at [redacted] Canada; [redacted] USA; Merck Research Laboratories, West Point, Pennsylvania, USA; or [redacted] USA. The USA and Canada are members of OECD and therefore part of the OECD Mutual Acceptance of Data system. GLP compliance statements are included in all GLP study reports.

Table 2.6.2: 12 Safety Pharmacology Studies with MOV (To Support ICH S7A and 7B Recommendations)

Study No. (GLP Status)	Study Title	Dose Levels (mg/kg)
TT # -7812 (GLP) [Sec. 2.6.3: 4].	Neuropharmacological Profile (NPP) of Orally Administered MOV in Rats	0, 50, 150, 500
TT # -7807 (GLP)[a] [Sec. 2.6.3: 4].	Effect of MOV on Cloned hERG Potassium Channels Expressed in Human Embryonic Kidney Cells	0, 30 µM (in vitro assay)
TT # -9400 (GLP)[b] [Sec. 2.6.3: 4].	Effect of NHC on Cloned hERG Potassium Channels Expressed in Human Embryonic Kidney Cells	0, 30, 100, 300 µM (in vitro assay)
TT # -7811 (GLP) [Sec. 2.6.3: 4].	Evaluation of Cardiovascular Function Following Oral Administration of MOV in Conscious Telemetered Beagle Dogs	0, 2, 6, 17
TT # -5603 Merck Research Laboratories (GLP) [Sec. 2.6.3: 4].	Oral Cardiovascular Telemetry Study in Beagle Dogs	0, 50
TT # -7813 (GLP) [Sec. 2.6.3: 4].	Pulmonary Assessment of Orally Administered MOV in the Conscious Rat	0, 50, 150, 500

= ; = ; EIDD-2801=MK-4482 or molnupiravir or MOV; GLP=Good Laboratory Practice; = ; hERG=human ether-à-go-go related gene; ICH=International Council for Harmonisation of Technical Requirements for Pharmaceuticals for Human Use; No.=number; SN = Study Number.

a: MOV hERG (TT # -7807): GLP

b: NHC hERG (TT # -9400): GLP

MOV was devoid of effects on CNS, respiratory, or cardiovascular functions in well-characterized safety pharmacology models. Detailed summaries of the individual studies are provided below. Nonclinical C_{max} exposure margins of NHC to humans were based on population pharmacokinetics analysis in adult patients with COVID-19 from P001 and P002 clinical trials (Part 1), where an 800 mg Q12H MOV dose resulted in systemic mean exposures C_{max} of 10.8 µM. The MOV C_{max} exposure margins at the NOEL for the in vivo safety pharmacology studies were ≥500 mg/kg in rats (23-fold higher than the human MOV C_{max} of 0.026 µM) or ≥50 mg/kg in dogs (322-fold higher than the human MOV C_{max} of

0.026 µM), extrapolated from the TK data for males in the respective 28-day studies in rats or dogs.

4.1 Neuropharmacological Profile (NPP) of Orally Administered MOV in Rats (TT #[redacted]-7812)

The purpose of this study was to evaluate the potential neuropharmacological effects of MOV administered orally in rats [Sec. 2.6.3: 4]. Three groups of 10 male SD rats each were administered MOV at a single oral (gavage) dose of 50, 150, or 500 mg/kg. An additional group of 10 rats was administered the vehicle (1% methylcellulose in deionized water). The dosing volume was 10 mL/kg. The rats were observed for neuropharmacological or other clinical signs using a modified Irwin/Functional Observational Battery test at 30 minutes and 1, 2, 4, 8, and 24 hours following treatment. Body temperature was measured at 1 hour following dose administration.

No neuropharmacological or clinical signs were observed through 24 hours postdose in any rats receiving either vehicle or MOV at 50, 150, or 500 mg/kg. There were no test article-related changes in body temperature at any dose tested.

The oral administration of MOV at doses of 50, 150, or 500 mg/kg did not produce any test article-related neuropharmacological effects or changes in body temperature in male rats. The NOEL after a single oral dose in male rats for neuropharmacological and body temperature, effects was ≥500 mg/kg (NHC C_{max} exposure 16-fold the NHC clinical C_{max} at the 800 mg Q12H human dose (extrapolated from TK data for males from the 28-day toxicity study; Nonclinical Study Report TT #[redacted]-7814).

4.2 MOV: Effect on hERG Current (TT #[redacted]-7807)

The objective of this study was to examine the in vitro effects of MOV on the hERG channel current (a surrogate for IKr, the rapidly activating delayed rectifier cardiac potassium current) [Sec. 2.6.3: 4].

MOV was applied to HEK-293 cells stably expressing hERG channel with manual patch clamp technique. The cells were exposed to MOV at 0 µM (corresponds to the reference control) and 30 µM, respectively. The hERG IKr currents were inhibited by 17.50 ± 8.84 % at 30 µM. The IC_{50} value of MOV was estimated to be greater than 30 µM (>1000-fold the MOV clinical C_{max} [0.026 µM] at the 800 mg Q12H dose).

4.3 NHC: Effect on Cloned hERG Potassium Channels Expressed in Human Embryonic Kidney Cells (TT #[redacted]-9400)

The objective of this study was to examine the in vitro effects of NHC on the hERG channel current (a surrogate for IKr, the rapidly activating delayed rectifier cardiac potassium current) [Sec. 2.6.3: 4].

Upon application of NHC, hERG current was reduced by (Mean ± SEM) 4.1 ± 2.4% at 30 µM (n = 4), 3.0 ± 2.9% at 100 µM (n = 5) and 1.8 ± 2.6% at 300 µM (n = 4) versus 3.7 ±

[redacted]

1.6% (n = 4) in control. hERG current reduction at all concentrations was not statistically significant ($p < 0.05$) when compared to vehicle control values. As greater than 50% inhibition was not observed at the highest concentration, the IC_{50} for the inhibitory effect of NHC on hERG potassium current was not calculated but was estimated to be greater than 300 µM. As an IC_{50} value was not determined, the IC_{20} for the inhibitory effect of NHC on hERG potassium current was not calculated but was estimated to be greater than 300 µM. The positive control article, cisapride, inhibited hERG potassium current by (Mean ± SEM; n = 5) 46.7 ± 1.2% at 30 nM and 80.7 ± 1.1% at 100 nM. This result confirms the sensitivity of the test system to hERG inhibition.

Overall, in this hERG assay, hERG current was not statistically significantly reduced ($p < 0.05$) at any NHC concentration tested (30, 100, 300 µM), when compared to vehicle control values. The IC_{50} value of NHC on hERG current was greater than 300 µM (28-fold above the NHC clinical C_{max} at the 800 mg Q12H dose).

4.4 Evaluation of Cardiovascular Function Following Oral Administration of MOV in Conscious Telemetered Beagle Dogs (TT #[redacted]-7811)

The purpose of this study was to determine the potential acute effects of MOV, after oral administration, on cardiovascular function in conscious telemetered beagle dogs [Sec. 2.6.3: 4].

Using a Latin Square design, 4 male non-naive beagle dogs each received vehicle alone (1.0% (w/v) methylcellulose in deionized water) and 3 doses of MOV (2, 6, and 17 mg/kg) by oral gavage at a dose volume of 2 mL/kg. Animals were observed for clinical signs predose, immediately postdose, and approximately 24 hours postdose administration. A single dose was administered on the day of dosing and a washout period of seven days was allowed between doses. One-minute means of hemodynamic parameters as well as ECG parameters and body temperature were measured for a period of at least 24 hours. One minute-tracings of the ECGs were obtained at 15 minutes prior to dosing and at 30 minutes, 1, 2, 4, 8, 12, and 24 hours postdose.

There were no test article-related clinical signs. The oral administration of MOV at doses of 2, 6, and 17 mg/kg did not induce any changes in body temperature, BP parameters (SBP, DBP, or MBP), HR, ECG parameters (RR, PR, or QRS intervals), or QT-related measured parameters (QT, QTci intervals).

The NOEL after a single oral dose in conscious, adult, telemetered beagle dogs for cardiovascular and BT effects was ≥17 mg/kg (1.4-fold the NHC C_{max} of 10.8 µM at the 800 mg Q12H human dose, extrapolated from the TK data for males in the 28-day toxicity study in dogs; Nonclinical Study Report TT #[redacted]-7815) [Sec. 2.6.3: 4].

4.5 MOV: Oral Cardiovascular Telemetry Study in Beagle Dogs (TT #[redacted]-5603)

MOV was administered orally at a single dose of 50 mg/kg to conscious, adult, telemetered beagle dogs to determine effects on cardiovascular function and BT continuously recorded for a 24-hour period [Sec. 2.6.3: 4].

[redacted]

Four male beagle dogs received a single oral dose of the vehicle alone (1.0% (w/v) methylcellulose in deionized water) followed by a single oral dose of 50 mg/kg of MOV in vehicle at a dose volume of 2 mL/kg. Arterial BP parameters (SBP, DBP, and MBP), HR, electrocardiographic parameters (PR, QRS, QT, and RR intervals), and BT were continuously recorded via telemetry for 24 hours postdose. The QT interval was corrected for HR variation using an individual animal correction method (QTci interval) and log-transformed QT:RR plots with a regression analysis were constructed for the time-matched vehicle/control and test article dose for assessment of the effects of MOV on QT interval independent of HR variation.

There were no test article-related clinical signs.

There were no test article-related changes observed in any BP parameters (SBP, DBP, or MBP), HR, ECG parameters (RR, PR, or QRS intervals), QT-related measured parameters (QT, QTci intervals, or QT:RR interval relationship), or BT following administration of 50 mg/kg of MOV.

The NOEL after a single oral dose in conscious, adult, telemetered beagle dogs for cardiovascular and BT effects was ≥50 mg/kg (5-fold the NHC C_{max} of 10.8 µM at the 800 mg Q12H human dose, extrapolated from the TK data for males in the 28-day toxicity study in dogs; Nonclinical Study Report TT #[redacted]-7815) [Sec. 2.6.3: 4].

4.6 Pulmonary Assessment of Orally Administered MOV in the Conscious Rat (TT #[redacted]-7813)

The purpose of this study was to determine the potential effects of MOV, administered orally, on respiratory rate, tidal volume, and minute volume in the conscious rat [Sec. 2.6.3: 4].

Twenty-four male rats (6/group) were trained for 2 days in the head-out plethysmograph chamber for approximately 15 to 30 minutes each, prior to the experiment. On the day of dosing, each animal was weighed and placed in the plethysmograph chamber and baseline respiratory parameters were obtained for 5 minutes following an approximately 5-minute stabilization period. The rats were then removed from the chamber and dosed by oral gavage at doses of 0 , 50, 150, or 500 mg/kg of MOV in vehicle (1% methylcellulose in deionized water) at a dose volume of 10 mL/kg. Following dosing, each animal was returned to its designated plethysmograph chamber and the respiratory parameters were recorded at 30 minutes (± 3 minutes), 1, 2, and 4 hours (±5 minutes). Animals were allowed to stabilize in the plethysmograph chamber for at least 5 minutes before each reading was taken. The following parameters were acquired, recorded and analyzed using Ponemah Physiology Platform (Ponemah v.5.20 Pulmonary): respiratory rate, tidal volume, and minute volume.

The oral administration of MOV at 50, 150, and 500 mg/kg did not produce any test article-related changes in respiratory rate, tidal volume, or minute volume. The NOEL for respiratory effects in male rats after a single oral dose was ≥500 mg/kg (NHC exposure 16-fold above the NHC C_{max} of 10.8 µM at the 800 mg Q12H human dose, extrapolated from

TK data for males from the 28-day toxicity study in rats; Nonclinical Study Report TT #[redacted]-7814) [Sec. 2.6.3: 4].

5 PHARMACODYNAMIC DRUG INTERACTIONS

5.1 Impact of Drug Combination on Antiviral Activity

To determine the potential effect of drug combinations on the antiviral activity against SARS-CoV-2, in vitro two-drug combination studies were performed (Nonclinical Study Report PD005) [Sec. 2.6.3: 1]. NHC was evaluated alone and in combination across a range of concentrations with 3TC, abacavir, FTC, hydroxychloroquine, nelfinavir, remdesivir, ribavirin, sofosbuvir, or tenofovir. Antiviral activity against SARS-CoV-2 was determined for each compound alone and in combination by measuring the reduction of the SARS-CoV-2 cytopathic effect on infected Vero cells. NHC, nelfinavir, and remdesivir when tested alone demonstrated antiviral activity with EC_{50} values of 1 µM, 0.7 µM, and 1.7 µM, respectively [Table 2.6.2: 13]. No cytotoxicity was observed for any compound tested (CC_{50} >20 µM) with the exception of nelfinavir, which was cytotoxic at high concentrations (CC_{50} = 11 µM). Neither synergy nor antagonism was observed for antiviral activity in vitro against SARS-CoV-2 for NHC in combination with 3TC, abacavir, FTC, hydroxychloroquine, nelfinavir, remdesivir, ribavirin, sofosbuvir, or tenofovir.

[redacted]

Table 2.6.2: 13 Evaluation of Drug Combination Impact on Antiviral Activity and Cytotoxicity in a SARS-CoV-2 Infection Assay

Compound	Cytotoxicity to Vero E6 Cells [a]	Antiviral Activity [b]	Assessment of Synergy/Antagonism in Antiviral Assay		
	CC_{50} (µM)	EC_{50} (µM)	Number of synergistic/ antagonistic doses [c]	Number of synergistic/ antagonistic doses [d]	Outcome
NHC	>20	1	0/1 [e]	0/1 [e]	NA
3TC	>20	>20	0/0	0/0	Neither synergy nor antagonism observed
Abacavir	>20	>20	0/0	0/0	
FTC	>20	>20	0/0	0/0	
Hydroxychloroquine	>20	>20	1/0	1/0	
Nelfinavir	11	0.7	0/2	0/0	
Remdesivir	>20	1.7	0/0	0/0	
Ribavirin	>20	>20	0/0	0/0	
Sofosbuvir	>20	>20	0/0	0/0	
Tenofovir	>20	>20	0/0	0/0	

Abbreviations: 3TC=lamivudine; CC_{50}=half-maximal cytotoxicity concentration; EC_{50}=half-maximal effective concentration; FTC=emtricitabine; µM=micromolar; NA=not applicable; NHC=EIDD-1931 or N-hydroxycytidine; SARS-CoV-2=severe acute respiratory syndrome-associated coronavirus-2.

[a] Single compound cytotoxicity on Vero E6 cells.

[b] Single compound antiviral activity in the SARS-CoV-2 infection assay.

[c] The number of synergistic (first value) or antagonistic (second) data points observed of 42 combinations. Synergy/antagonism defined as z-score of delta-Bliss of >3 or <-3, respectively. This value represents $p<0.01$ assuming normal and independent errors. Since data may not be normal and points not independent, control experiment NHC crossed with NHC is used to set threshold for significance. See also footnote e.

[d] The number of synergistic (first value) or antagonistic (second) data points excluding cytotoxic doses (>50% loss of viability).

[e] Combination results reported for negative control cross-titration in which NHC was titrated against itself.

Source: Nonclinical Study Report PD005 [Sec. 2.6.3: 1].

6 DISCUSSION AND CONCLUSIONS

MOV is developed for the treatment of patients with COVID-19. MOV is a 5′-isobutyrate ester prodrug designed to be rapidly metabolized by serum/cellular esterases to deliver the nucleoside metabolite NHC into systemic circulation following oral administration. NHC-TP incorporation (as NHC-MP) into SARS-CoV-2 RNA by the viral RNA polymerase (nsp12) results in an accumulation of errors in the viral genome leading to inhibition of replication. The mechanism of action is known as viral error catastrophe or viral lethal mutagenesis.

Primary pharmacology studies demonstrating the antiviral activity of MOV/NHC against SARS-CoV-2 and other RNA viruses were conducted in vitro and in mouse, guinea pig,

hamster, and ferret models of viral infection. NHC demonstrated specific, dose-dependent inhibition of viral replication with sub- to low-micromolar EC_{50} values against SARS-CoV-2, SARS-CoV-1, and MERS-CoV in multiple cell types. MOV/NHC shows broad-spectrum antiviral activity in vitro against multiple viruses including CoV, influenza A (pandemic and seasonal) and influenza B strains, as well as against highly pathogenic H5N1 and H7N9 strains, togaviruses (genus alphavirus) VEEV, EEEV, and CHKV, and Ebola virus.

NHC was equally effective against SARS-CoV-2 variants of concern B.1.1.7 (Alpha), B.1.351 (Beta), P.1 (Gamma), B.1.617.2 (Delta), B.1.1.529 (Omicron), and Omicron BA.1.1, variant of interest C.37 (Lambda), and variant being monitored B.1.621 (Mu) compared with the WA1 isolate in a cytopathic effect protection assay in Vero E6 cells.

NHC was also active against coronaviruses that have mutations which reduce susceptibility to remdesivir in cell culture assays. NHC was active against SARS-CoV-2 replicons with remdesivir resistance-associated amino acid substitutions in NSP12 (polymerase) and MOV treatment-emergent NSP12 and NSP14 (exonuclease) variants in a reporter replicon assay.

NHC was efficiently taken up by cell lines, PBMCs, and HBEC air-liquid interface cultures, and phosphorylated to mono-, di-, and tri-phosphate forms. NHC was phosphorylated to NHC-TP in a dose-dependent manner in human, dog, and rat PBMCs. The phosphorylated forms of NHC were catabolized in a few hours in cell lines and PMBCs after 24 hours of treatment with NHC. NHC-TP was rapidly metabolized in HBEC air-liquid interface cultures by 24 hours after removal of NHC, with NHC-TP concentrations higher than for NHC-DP or NHC-MP. NHC-TP was detectable at least 24 hours after treatment with 10 µM NHC in HBEC air-liquid interface cultures.

MOV (500 mg/kg) significantly reduced infectious SARS-CoV-2 levels in lung tissue from LoM when administered 12 hours prior, 24 hours post, or 48 hours post direct infection of human lung tissue, followed by twice daily dosing thereafter. In a ferret model, treatment with twice daily (5 mg/kg) MOV reduced SARS-CoV-2 infectious viral titers in nasal secretions from infected ferrets and suppressed all viral transmission to the untreated direct contacts, despite prolonged direct proximity between source and contact animals. In a Syrian hamster model of SARS-CoV-2 infection and disease, MOV prophylactic or therapeutic treatment showed decreased viral RNA titers and infectious virus from lungs several days post infection. In a Syrian hamster model of SARS-CoV-2 infection and disease using either the B.1-G (Wuhan strain), B.1.1.7 (Alpha), or B.1.351 (Beta) variants of SARS-CoV-2, treatment with MOV resulted in statistically significant reductions in viral RNA in lungs and in infectious virus lung titers regardless of variant.

Antiviral activity of MOV was also observed in animal infection models of SARS-CoV-1, MERS-CoV, and influenza. MOV (500 mg/kg) provided therapeutic efficacy when administered 24 hours after infection with SARS-CoV-1 and 12 hours after infection with MERS-CoV in a mouse model.

Prolonged in vitro exposure treatment (14 days) of CEM and HepG2 cells with MOV did not result in mitochondrial toxicity or dysfunction. Neither MOV nor NHC exhibited off-target

activities of clinical concern. NHC-TP had calculated IC_{50} values >1000 μM under physiological concentrations of dNTPs for human DNA polymerases α, β, and γ.

MOV was devoid of effects on CNS, respiratory, or cardiovascular functions in well-characterized safety pharmacology models.

There was no impact on the in vitro antiviral activity of NHC against SARS-CoV-2 in two-drug combination studies with 3TC, abacavir, FTC, hydroxychloroquine, nelfinavir, remdesivir, ribavirin, sofosbuvir, or tenofovir.

Collectively, the results from the nonclinical pharmacodynamic and safety pharmacology studies conducted with MOV support use of MOV for treatment of adult patients with COVID-19.

7 LIST OF REFERENCES

[Ref. 4.3: 05JF05] Agostini ML, Pruijssers AJ, Chappell JD, Gribble J, Lu X, Andres EL, et al. Small-molecule antiviral beta-D-N(4)-hydroxycytidine inhibits a proofreading-intact coronavirus with a high genetic barrier to resistance. J Virol. 2019 Dec;93(24):e01348-19.

[Ref. 4.3: 05JF06] Flavell RA, Sabo DL, Bandle EF, Weissmann C. Site-directed mutagenesis: generation of an extracistronic mutation in bacteriophage Qbeta RNA. J Mol Biol. 1974;89:255-72.

[Ref. 4.3: 05JF07] Hernandez-Santiago BI, Beltran T, Stuyver L, Chu CK, Schinazi RF. Metabolism of the anti-hepatitis C virus nucleoside beta-D-N(4)-hydroxycytidine in different liver cells. Antimicrob Agents Chemother. 2004 Dec;48(12):4636-42.

[Ref. 4.3: 05JF08] Mullins JI, Heath L, Hughes JP, Li D, Essigmann JM, Harris KS, et al. Mutations based on viral decay acceleration in the HIV-1 genomes of a clinical population treated with the mutagenic nucleoside KP1461. Retrovirology. 2011 Oct 3;8(suppl 2):P84.

[Ref. 4.3: 05JF09] Toots M, Yoon JJ, Hart M, Natchus MG, Painter GR, Plemper RK. Quantitative efficacy paradigms of the influenza clinical drug candidate EIDD-2801 in the ferret model. Transl Res. 2020 Apr;218:16-28.

[Ref. 4.3: 05JF0B] Sticher ZM, Lu G, Mitchell DG, Marlow J, Moellering L, Bluemling GR, et al. Analysis of the potential for N(4)-hydroxycytidine to inhibit mitochondrial replication and function. Antimicrob Agents Chemother. 2020 Feb;64(2):e01719-19.

[Ref. 4.3: 05JF0D] Toots M, Yoon JJ, Cox RM, Hart M, Sticher ZM, Makhsous N, et al. Characterization of orally efficacious influenza drug with high resistance barrier in ferrets and human airway epithelia. Sci Transl Med. 2019 Oct 23;11:eaax5866.

[Ref. 4.3: 05JF0F] Urakova N, Kuznetsova V, Crossman DK, Sokratian A, Guthrie DB, Kolykhalov AA, et al. Beta-D-N(4)-hydroxycytidine is a potent anti-alphavirus compound that induces a high level of mutations in the viral genome. J Virol. 2018 Feb;92(3):e01965-17.

[Ref. 4.3: 05JF0G] Yoon JJ, Toots M, Lee S, Lee ME, Ludeke B, Luczo JM, et al. Orally efficacious broad-spectrum ribonucleoside analog inhibitor of influenza and respiratory syncytial viruses. Antimicrob Agents Chemother. 2018 Aug;62(8):e00766-18.

[Ref. 4.3: 05JM4T] Painter GR, Bowen RA, Bluemling GR, DeBergh J, Edpuganti V, Gruddanti PR, et al. The prophylactic and therapeutic activity of a broadly active ribonucleoside analog in a murine model of intranasal venezuelan equine encephalitis virus infection. Antiviral Res. 2019;171:104597.

[Ref. 4.3: 05K5RM] Agostini ML, Andres EL, Sims AC, Graham RL, Sheahan TP, Lu X, et al. Coronavirus susceptibility to the antiviral remdesivir (GS-5734) is mediated by the viral polymerase and the proofreading exoribonuclease. mBio. 2018;9:e00221-18. doi: 10.1128/mBio.00221-18.

[Ref. 4.3: 05K8L0] Sheahan TP, Sims AC, Zhou S, Graham RL, Pruijssers AJ, Agostini ML, et al. An orally bioavailable broad-spectrum antiviral inhibits SARS-CoV-2 in human airway epithelial cell cultures and multiple coronaviruses in mice. Sci Transl Med. 2020;12, eabb5883. doi: 10.1126/scitranslmed.abb5883.

[Ref. 4.3: 05NRF7] Cox RM, Wolf JD, and Plemper RK. Therapeutically administered ribonucleoside analogue MK-4482/EIDD-2801 blocks SARS-CoV-2 transmission in ferrets. Nat Microbiol (2020). https://doi.org/10.1038/s41564-020-00835-2.

[Ref. 4.3: 05R3LW] Rosenke K, Hansen F, Schwarz B, Feldmann F, Haddock E, Rosenke R, et al. Orally delivered MK-4482 inhibits SARS-CoV-2 replication in the Syrian hamster model. Preprint. Res Sq. 2020;rs.3.rs-86289. Published 2020 Oct 8. doi:10.21203/rs.3.rs-86289/v1.

[Ref. 4.3: 05R3M7] Szemiel AM, Merits A, Orton RJ, MacLean O, Pinto RM, Wickenhagen A, et al. In vitro evaluation of remdesivir resistance reveals genome plasticity of SARS-CoV-2. bioRxiv 2021.02.01.429199; doi: https://doi.org/10.1101/2021.02.01.429199.

[Ref. 4.3: 05R3M8] Wahl A, Gralinski LE, Johnson CE et al. SARS-CoV-2 infection is effectively treated and prevented by EIDD-2801. Nature (2021). https://doi.org/10.1038/s41586-021-03312-w.

[Ref. 4.3: 06CK43] Reynard O, Nguyen XN, Alazard-Dany N, Barateau V, Cimarelli A, Volchkov VE. Identification of a new Ribonucleoside inhibitor of Ebola virus replication. Viruses. 2015;7:6233-40. Erratum in: Viruses. 2016;8:137.

[Ref. 4.3: 06FDKT] He X, Quan S, Xu M, Rodriguez S, Goh SL, Wei J, et al. Generation of SARS-CoV-2 reporter replicon for high-throughput antiviral screening and testing. PNAS Apr 2021, 118 (15) e2025866118; DOI: 10.1073/pnas.2025866118.

[Ref. 4.3: 06FGX5] Abdelnabi R, Foo CS, De Jonghe S, Maes P, Weynand B, Neyts J. Molnupiravir inhibits the replication of the emerging SARS-CoV-2 variants of concern (VoCs) in a hamster infection model. (Accepted Manuscript) J Infectious Diseases, 2021;jiab361, https://doi.org/10.1093/infdis/jiab361.

[redacted]

[Ref. 4.3: 06FP3F] Martinot M, Jary A, Fafi-Kremer S, Leducq V, Delagreverie H, Garnier M, Pacanowski J, Mekinian A et al. Remdesivir failure with SARS-CoV-2 RNA-dependent RNA-polymerase mutation in a B-cell immunodeficient patient with protracted Covid-19 [published online ahead of print, 2020 Sep 28]. Clin Infect Dis. 2020;ciaa1474. doi:10.1093/cid/ciaa1474.

[Ref. 4.3: 06FR0T] MK-4482: [redacted] Data Reports for EIDD-1931 (NHC)

[Ref. 4.3: 06FRN8] Iketani S, Forouhar F, Liu H, Hong SJ, Lin FY, Nair MS, et al. Lead compounds for the development of SARS-CoV-2 3CL protease inhibitors. Nat Commun. 2021 Apr 1;12(1):2016.

[Ref. 4.3: 06FRNB] Liu L, Wang P, Nair MS, Yu J, Rapp M, Wang Q, et al. Potent neutralizing antibodies against multiple epitopes on SARS-CoV-2 spike. Nature. 2020 Aug;584(7821):450-456.

[Ref. 4.3: 06G338] Kabinger F, Stiller C, Schmitzová J, Dienemann C, Kokic G, Hillen HS, et al. Mechanism of molnupiravir-induced SARS-CoV-2 mutagenesis. Nat Struct Mol Biol. 2021 Aug 11.

[Ref. 4.3: 06G33J] Gordon CJ, Tchesnokov EP, Schinazi RF, Götte M. Molnupiravir promotes SARS-CoV-2 mutagenesis via the RNA template. J Biol Chem. 2021 Jul;297(1):100770.

[Ref. 4.3: 07YGG0] Dabrowska A, Szczepanski A, Botwina P, Mazur-Panasiuk N, Jiřincová H, Rabalski L, et al. Efficacy of antiviral drugs against the omicron variant of SARS-CoV-2. bioRxiv 2021.12.21.473268; doi: https://doi.org/10.1101/2021.12.21.473268.

[Ref. 4.3: 07YJSK] Rosales R, McGovern BL, M. Rodriguez L, Rai DK, Cardin RD, Anderson AS, et al. Nirmatrelvir, Molnupiravir, and Remdesivir maintain potent in vitro activity against the SARS-CoV-2 Omicron variant. bioRxiv 2022.01.17.476685; doi: https://doi.org/10.1101/2022.01.17.476685.

[Ref. 4.3: 07YKW6] Li P, Wang Y, Lavrijsen M, Lamers MM, de Vries AC, Rottier RJ, et al. SARS-CoV-2 Omicron variant is highly sensitive to molnupiravir, nirmatrelvir, and the combination. Cell Res. 2022 Jan 20. doi: 10.1038/s41422-022-00618-w. Epub ahead of print. PMID: 35058606.

[Ref. 4.3: 07YNFR] Vangeel L, Chiu W, De Jonghe S, Maes P, Slechten B, Raymenants J, et al. Remdesivir, Molnupiravir and Nirmatrelvir remain active against SARS-CoV-2 Omicron and other variants of concern. Antiviral Res. 2022 Jan 24;198:105252. doi: 10.1016/j.antiviral.2022.105252.

[redacted]

[Ref. 4.3: 07YNGB] Bojkova D, Widera M, Ciesek S, Wass MN, Michaelis M, Cinatl J Jr. Reduced interferon antagonism but similar drug sensitivity in Omicron variant compared to Delta variant of SARS-CoV-2 isolates. Cell Res. 2022 Jan 21:1–3. doi: 10.1038/s41422-022-00619-9. Epub ahead of print. PMID: 35064226; PMCID: PMC8781709.

[Ref. 4.3: 07YNH8] Takashita E, Kinoshita N, Yamayoshi S, Sakai-Tagawa Y, Fujisaki S, Ito M, et al. Efficacy of Antibodies and Antiviral Drugs against Covid-19 Omicron Variant. N Engl J Med. 2022 Jan 26. doi: 10.1056/NEJMc2119407. Epub ahead of print. PMID: 35081300.

TABLE OF CONTENTS

TABLE OF CONTENTS 1
Sec. 2.6.3.1 Pharmacology: Overview 2
Sec. 2.6.3.2 Primary Pharmacodynamics 8
Sec. 2.6.3.3 Secondary Pharmacodynamics 9
Sec. 2.6.3.4 Safety Pharmacology 10
Sec. 2.6.3.5 Pharmacodynamic Drug Interactions 11

[redacted]

C Confidential

Sec. 2.6.3.1 Pharmacology: Overview

Test Article: Molnupiravir

Type of Study	Test System	Method of Administration	Testing Facility	Study Number	Location
Primary Pharmacodynamics					
Defining Efficacy and Cytotoxicity for SARS-CoV Infected Human Lung cells Treated with EIDD-1931	In vitro	NA	[redacted] USA	PD001 EIDD Report 25.038	[Ref. 4.2.1.1: PD001 MK4482]
In Vitro Evaluation of One Test Compound (EIDD-2801) on Human Myeloid and Erythroid Colony Forming Cell Assays (EMY-05)	In vitro	NA	[redacted] USA	PD006	[Ref. 4.2.1.1: PD006 MK4482]
In Vitro Assessment of Antiviral Activity of MK-4482 and N-Hydroxycytidine in Multiple Susceptible Cell Lines	In vitro	NA	Merck Research Laboratories[a], West Point, Pennsylvania, USA [redacted] USA [redacted] USA [redacted] USA [redacted] USA	PD007	[Ref. 4.2.1.1: PD007 MK4482]

[redacted]

Test Article: Molnupiravir

Type of Study	Test System	Method of Administration	Testing Facility	Study Number	Location
Primary Pharmacodynamics (continued)					
In Vitro Antiviral Activity of N-hydroxycytidine Against SARS-CoV-2 And Other Viruses	In vitro	NA	Merck Research Laboratories[a], West Point, Pennsylvania, USA [redacted] USA	PD008	[Ref. 4.2.1.1: PD008 MK4482]
In Vitro Cytotoxicity Evaluations of Compounds MK595 and MK596, [redacted] Study SE141853	In vitro	NA	[redacted] USA	PD009	[Ref. 4.2.1.1: PD009 MK4482]
Evaluation of N-Hydroxycytidine Antiviral Activity Against SARS-CoV-2 Variants in Vero Cells	In vitro	NA	[redacted] USA Merck Research Laboratories[a], West Point, Pennsylvania, USA	PD010	[Ref. 4.2.1.1: PD010 MK4482]
Evaluation of N-Hydroxycytidine Antiviral Activity Against SARS-CoV-2 Variants Lambda and Mu in Vero Cells	In vitro	NA	[redacted] USA Merck Research Laboratories[a], West Point, Pennsylvania, USA	PD014	[Ref. 4.2.1.1: PD014 MK4482]

[redacted]

C Confidential

Test Article: Molnupiravir

Type of Study	Test System	Method of Administration	Testing Facility	Study Number	Location
Evaluation of N-Hydroxycytidine Antiviral Activity Against the SARS-CoV-2 Omicron Variant in Vero Cells	In vitro	NA	[redacted] USA Merck Research Laboratories[a], West Point, Pennsylvania, USA	PD015	[Ref. 4.2.1.1: PD015 MK4482]
Evaluation of Amino Acid Substitutions in SARS-CoV-2 NSP12 (Polymerase) and NSP14 (Exonuclease) on the Antiviral Activity of N-Hydroxycytidine in a Replicon Model	In vitro	NA	Merck Research Laboratories[a], West Point, Pennsylvania, USA	PD011	[Ref. 4.2.1.1: PD011 MK4482]
In Vitro Evaluation of NHC Uptake By Cell Lines, By Human, Dog, and Rat Peripheral Blood Mononuclear Cells, and In Human Bronchial Epithelial Cell (HBEC) Air-liquid Interface (ALI) Cultures	In vitro	NA	Merck Research Laboratories[a], West Point, Pennsylvania, USA Merck Research Laboratories, Cambridge, Massachusetts, USA	PD012	[Ref. 4.2.1.1: PD012 MK4482]
Efficacy of Orally Administered EIDD-01931 in the Intraperitoneal Ebolavirus Challenge BALB/c Mouse Model - Study 3	Mouse/ BALB/c	Oral (gavage)	[redacted] USA	PD002 [redacted] STDY-16-0019-JC	[Ref. 4.2.1.1: PD002 MK4482]

[redacted]

Test Article: Molnupiravir

Type of Study	Test System	Method of Administration	Testing Facility	Study Number	Location
Secondary Pharmacodynamics					
[redacted] Data Report	In vitro	NA	[redacted] USA	PD003 [redacted] SN: EMO022216-1	[Ref. 4.2.1.2: PD003 MK4482]
Assessment of the Off-target Activity of MK 4482 and N-hydroxycytidine in a Panel of Enzyme, Radioligand Binding, and Functional Assays	In vitro	NA	Merck Research Laboratories[a], West Point, Pennsylvania, USA	PD004	[Ref. 4.2.1.2: PD004 MK4482]
Determination of the Effect of N-Hydroxycytidine Triphosphate on the Activity of Human DNA Polymerases Alpha, Beta, and Gamma	In vitro	NA	Merck Research Laboratories[a], Kenilworth, New Jersey, USA	PD013	[Ref. 4.2.1.2: PD013 MK4482]

[redacted]

C Confidential

Sec. 2.6.3.1 Pharmacology: Overview (Continued)

Test Article: Molnupiravir

Type of Study	Test System	Method of Administration	Testing Facility	Study Number	Location
Safety Pharmacology					
Neuropharmacological Profile (NPP) of Orally Administered MOV in Rats	Rat/ Crl:CD(SD)	Oral (gavage)	[redacted] USA	TT # [redacted]-7812 [b]	[Ref. 4.2.1.3: TT[redacted]78 12FIN]
Effect of MOV on Cloned hERG Potassium Channels Expressed in Human Embryonic Kidney Cells	In vitro	NA	[redacted] Canada	TT # [redacted]-7807 [b]	[Ref. 4.2.1.3: TT[redacted]78 07FIN]
Effect of NHC on Cloned hERG Potassium Channels Expressed in Human Embryonic Kidney Cells	In vitro	NA	[redacted] USA	TT # [redacted]-9400 [b]	[Ref. 4.2.1.3: TT[redacted]94 00FIN]
Evaluation of Cardiovascular Function Following Oral Administration of MOV in Conscious Telemetered Beagle Dogs	Dog/beagle	Oral (gavage)	[redacted] USA	TT # [redacted]-7811 [b]	[Ref. 4.2.1.3: TT[redacted]78 11FIN]
Oral Cardiovascular Telemetry Study in Beagle Dogs	Dog/beagle	Oral (gavage)	Merck Research Laboratories[a], West Point, Pennsylvania USA	TT # [redacted]-5603 [b]	[Ref. 4.2.1.3: TT[redacted]56 03FIN]
Pulmonary Assessment of Orally Administered MOV in the Conscious Rat	Rat/ Crl:CD(SD)	Oral (gavage)	[redacted] USA	TT # [redacted]-7813 [b]	[Ref. 4.2.1.3: TT[redacted]78 13FIN]

[redacted]

C Confidential

Sec. 2.6.3.1 Pharmacology: Overview (Continued)

Test Article: Molnupiravir

Type of Study	Test System	Method of Administration	Testing Facility	Study Number	Location
Pharmacodynamic Drug Interactions					
In Vitro Assessment of Antiviral Activity of N-hydroxycytidine and the Impact of Two-drug Combinations	In vitro	NA	Merck Research Laboratories[a], West Point, Pennsylvania, USA [redacted] USA	PD005	[Ref. 4.2.1.4: PD005 MK4482]

ALI=air-liquid interface; GLP=Good Laboratory Practice; HBEC=human bronchial epithelial cell; hERG=human ether-à-go-go-related gene; MOV=molnupiravir or MK-4482 or EIDD-2801 or MK595; NA=Not applicable; NHC=EIDD-1931 or N-hydroxycytidine or MK596; NPP=Neuropharmacological Profile; NSP=nonstructural protein; SD=Sprague-Dawley; SN=study number; USA=United States of America.

a Merck Research Laboratories is a division of Merck, Sharp & Dohme Corp. (MSD).

b Report contains a GLP compliance statement.

[redacted]

C Confidential

Sec. 2.6.3.2 Primary Pharmacodynamics

See Primary Pharmacodynamics [Sec. 2.6.2: 2].

[redacted]

C Confidential

Sec. 2.6.3.3 Secondary Pharmacodynamics

See Secondary Pharmacodynamics [Sec. 2.6.2: 3].

[redacted]

C Confidential

Sec. 2.6.3.4 Safety Pharmacology

Test Article: Molnupiravir

Organ Systems Evaluated	Species/ Strain	Method of Administration	Dose/Concentration Level[a]	Gender and No. per Group	Noteworthy Findings	GLP Compliance	Study Number
CNS	Rat/ Crl:CD(SD)	Oral (gavage)	0, 50, 150, 500 mg/kg	10 males	No MOV-related findings	Yes	TT #[redacted]-7812 [Ref. 4.2.1.3: TT [redacted]7812FIN]
hERG (MOV)	In vitro	NA	0, 30 µM	NA	The IC_{50} value of MOV was greater than 30 µM (>1000-fold above the MOV clinical C_{max} [0.026 µM] at the 800 mg Q12H dose)	Yes	TT #[redacted]-7807 [Ref. 4.2.1.3: TT [redacted]7807FIN]
hERG (NHC)	In vitro	NA	0, 30, 100, 300 µM	NA	The IC_{50} value of NHC was greater than 300 µM (28-fold above the NHC clinical C_{max} of 10.8 µM at the 800 mg Q12H dose).	Yes	TT #[redacted]-9400 [Ref. 4.2.1.3: TT [redacted]9400FIN]
CV	Dog/beagle	Oral (gavage)	0, 2, 6, 17 mg/kg	4 males	No MOV-related findings	Yes	TT #[redacted]-7811 [Ref. 4.2.1.3: TT [redacted]7811FIN]
CV	Dog/beagle	Oral (gavage)	0, 50 mg/kg	4 males	No MOV-related findings	Yes	TT #[redacted]-5603 [Ref. 4.2.1.3: TT [redacted]5603FIN]
Respiratory	Rat/ Crl:CD(SD)	Oral (gavage)	0, 50, 150, 500 mg/kg	6 males	No MOV-related findings	Yes	TT #[redacted]-7813 [Ref. 4.2.1.3: TT [redacted]7813FIN]

C_{max} = observed maximum concentration; CNS = Central nervous system; CV = Cardiovascular; GLP = Good Laboratory Practice; hERG = human ether-à-go-go-related gene; IC_{50} = half-maximal inhibitory concentration; MOV = molnupiravir or MK-4482 or EIDD-2801; NA = Not applicable; NHC = EIDD-1931 or N-hydroxycytidine; Q12H = every 12 hours; SD = Sprague-Dawley; SN = study number.

a NOEL for in vivo studies is underlined

[redacted]

Sec. 2.6.3.5 Pharmacodynamic Drug Interactions

See Pharmacodynamic Drug Interactions [Sec. 2.6.2: 5].

[redacted]